Estimating State Price Densities Implied by American Options*

Zhongjun Qu†

Boston University

Guang Zhang‡

Hong Kong University of Science and Technology (Guangzhou)

April 28, 2025

Abstract

We propose a new method to estimate state price densities implicit in American-style options. The method involves estimating the parameters of a Gauss-Hermite series expansion and solving a sequence of recursive equations for the early exercise premium. The resulting estimator can capture sudden shifts in density that may occur during financial crises or in response to significant policy events. It also provides an estimate of the early exercise premium that is of independent interest. We illustrate the proposed method using both calibrated simulations and empirical applications. Our findings indicate that the state price densities implied by S&P 500 ETF options can predict future returns up to a one-year horizon for the period 2009-2023. An application to individual stock options suggests that the state price densities have predictive power for future stock returns at both short (one month) and long (one year) horizons. The analysis also reveals a pattern of sign reversal when moving from short to longer horizon predictions.

Keywords: State price density, American option, early exercise premium, nonparametric.
JEL classification: C14, C22, G13.

*We are grateful to coeditor Atsushi Inoue, the associate editor, two anonymous referees, and Samuel Messer for helpful comments that improved the paper. Guang Zhang acknowledges the support from the Guangzhou-HKUST(GZ) Joint Funding Program (No.2024A03J0630). The authors have no competing interests to declare.

†Department of Economics, Boston University (qu@bu.edu).

‡Thrust of Financial Technology, Hong Kong University of Science and Technology (Guangzhou) (guangzhang@hkust-gz.edu.cn).

1 Introduction

Equilibrium prices of financial assets reflect both uncertainty and the market's collective preferences for potential payoffs. This relationship is captured by a State Price Density (SPD), in the form of a probability distribution. Intuitively, the SPD assigns weights to various economic states, with larger values indicating a higher probability and/or greater preference for positive asset returns in that state. SPDs are central to asset pricing theories, particularly in derivative pricing and term structure modeling. Their importance is also recognized by central banks, as SPDs provide predictive distributions that help offer insights into future economic conditions. For example, the Federal Reserve Bank of Minneapolis maintains SPD estimates across diverse markets, including commodities, equities, exchange rates, inflation, and interest rates.[1]

The options market is an ideal setting for estimating SPDs because (1) option contracts have simple payoff structures, (2) their strike prices cover a wide range of economic states, and (3) their maturities range from a few days to over a year, providing insights into different time horizons. In practice, index options are mainly European-style, with fixed exercise dates, while American-style options, allowing exercise anytime before expiration, are more common and apply to a broader range of assets. These include equities (e.g., individual stocks, market index futures, and ETFs); commodities (e.g., gold, silver, and agricultural products); energy (e.g., natural gas and crude oil); and fixed-income securities (e.g., Treasuries and European government bonds). Researchers often use American options to estimate SPDs for these assets.

Many methods exist to estimate SPDs using European-style options. These include: Jackwerth and Rubinstein's (1996) binomial tree-based approach; Jarrow and Rudd's (1982) and Longstaff's (1995) Gram-Charlier based estimator; Ait-Sahalia and Lo's (1998) and Dalderop's (2020) kernel-based estimators; Ait-Sahalia and Duarte's (2003) constrained local polynomial estimator; Shimko's (1993) global polynomial method; and Figlewski's (2010) spline method.

[1] Federal Reserve Bank of Minneapolis, "Current and Historical Market-Based Probabilities," https://www.minneapolisfed.org/banking/current-and-historical-market–based-probabilities.

As these methods were designed for European options, they do not account for the early exercise premium inherent in American options. Applying these methods directly to American options can therefore result in biased estimates, especially for horizons extending beyond a few months. Section 4 of this paper quantifies this bias through calibrated simulations. The empirical section, using actual data, further confirms that the bias can be substantial (see Figure 2 for a visual comparison and the empirical section for more details). These findings indicate the importance of considering the early exercise feature, especially in environments of high interest rates, as the early exercise premium for put options can be sizable under such conditions.

Few methods are available for estimating SPDs using American options. The two main approaches are Melick and Thomas's (1997) method, which approximates the price of an American option as a weighted average of upper and lower bounds related to European option prices, and Tian's (2011) method, which iteratively estimates the early exercise premium and the SPD using a binomial-tree model. In empirical studies, researchers often use Melick and Thomas's (1997) method or assume the early exercise premium is negligible and resort to methods designed for European options. However, the latter requires excluding in-the-money options or limiting the analysis to short horizons to reduce bias. There is a need for new methods that can estimate SPDs across both short and long horizons without discarding data and improve the understanding of the early exercise premium in this context.

This paper proposes a nonparametric estimator to estimate SPDs from American options. The approach combines a Gauss-Hermite series expansion with a recursive equation for the early exercise premium. The estimation involves determining the expansion coefficients and solving the recursive equation iteratively. It requires only a single cross-section of American option prices with a common maturity, a proxy for the risk-free rate, and an estimate of the dividend rate. Unlike methods that apply temporal smoothing, it can capture sudden shifts in the SPD, such as those caused by financial crises or major policy announcements. It is suitable for both low- and high-frequency data and provides an estimate of the early exercise premium of independent interest. The estimator generalizes Lu and Qu's (2021) method from European to American options, incorporating additional steps to account for the early exercise premium.

We evaluate the method's performance using empirically calibrated simulations and compare with the estimators of Melick and Thomas (1997) and Tian (2011). We then proceed to an empirical application with two objectives: to assess the proposed estimator's performance on real data and to evaluate whether the recovered SPD can predict future asset returns at various horizons. The first objective is challenging because most assets do not have European and American options, making it difficult to measure the early exercise premium. However, we identified a pair of assets that provide valuable insights: the S&P 500 index (SPX) and an ETF, SPY, designed to track the SPX; SPX options are European-style, while SPY options are American-style. This close connection allows us to treat SPY options as nearly equivalent to SPX options, with their price difference primarily reflecting the early exercise premium. As a result, the SPD derived from the SPX options can serve as a reference point for evaluating the accuracy of our method in recovering both the SPD and the early exercise premium.

The empirical results show that our methods effectively recover the SPDs because the estimates using SPY options closely mirror those using SPX. The findings also highlight the importance of accounting for the early exercise premium, especially at longer horizons. For example, using data from 02/17/2023, when the London Inter-Bank Offered Rate (LIBOR) was 5.6%, ignoring the early exercise premium results in a sizable estimation bias at the one-year horizon: the integrated mean squared error is 4.3E-2 when the early exercise feature is ignored, compared to 2.5E-3 when it is accounted for. Both estimates are computed relative to the SPD estimated directly from European options.

For the predictive analysis, we consider both mean and quantile regressions using a quantile of the SPD as the predictor for future returns. We present results for three sample periods to assess potential shifts in predictability due to extreme market conditions: a benchmark sample from 2009.06 to 2020.02, an extended sample that includes the COVID pandemic period (2009.06-2023.02), and a further extended sample which includes the 2008 financial crisis (2007.01-2023.02). For each sample period, we consider four different horizons, at approximately one month, three months, six months, and one year.

The predictive mean regressions show a statistically significant relationship (at the 10% level) for the first two sample periods. The evidence is clear at monthly to semi-annual horizons but becomes more mixed at the annual horizon. Lower quantiles consistently exhibit stronger predictive power than upper quantiles. Intuitively, large decreases in the lower quantiles are often triggered by negative market events, such as the onset of the COVID pandemic. Over the past 20 years, the market has typically recovered well from major declines. As a result, such shifts in lower quantiles often signal investment opportunities, which, on average, are associated with higher subsequent returns, particularly over longer horizons.

The predictive quantile regressions yield clear-cut results for the monthly, quarterly, and semi-annual horizons across all three sample periods. When a quantile above the median is used to predict the same quantile of the return distribution, the slope coefficients are often significant. Using a quantile below the median as the predictor often yields insignificant estimates. This asymmetry reflects the same intuition as in the mean regression case: because markets have generally rebounded from significant declines, actual outcomes often exceeded initial pessimistic expectations. In other words, lower quantiles of the SPD captured a fear or risk premium that was accompanied by stronger subsequent returns. These lower quantiles showed little correlation with the lower quantiles of the actual return distribution.

We also consider a second application where we estimate the SPDs implied by individual stock options and evaluate their predictive power for future returns over January 1996 to December 2021. The findings suggest that the SPDs have predictive power for future returns at both short (one month) and long (one year) horizons. The analysis also reveals a pattern of sign reversal when moving from short to longer horizons. Specifically, at the monthly horizon, the regression coefficients for the SPDs are mostly positive, while at the annual horizon, they are mostly negative. Explaining this reversal could be a topic of future studies.

Our empirical results contribute to the literature on whether and how information from the options market predicts stock returns. Bollerslev et al. (2011) show that the volatility risk premium predicts excess returns on the S&P500 index at monthly and quarterly horizons during 1990-2003. An et al. (2014) report that stocks with large prior increases in call (put) implied volatilities exhibit high (low) future returns, a pattern most evident at monthly horizons and persisting up to six months for 1996-2011. Xing et al. (2010) examine the predictability of implied volatility skewness of stock options from 1996-2005, finding that the predictability weakens after one month but can extend up to six months. Some studies use the tails of the SPD to forecast future returns; see Andersen et al. (2015) for parametric methods and Andersen et al. (2021) for nonparametric methods. By estimating SPDs from American options, our methods enable the evaluation of predictive power across a broader range of markets compared to approaches limited to European options.

The remainder of the paper is organized as follows: Section 2 overviews key concepts on American options. Section 3 introduces the estimator. Section 4 evaluates its performance through empirically calibrated simulations. Section 5 presents two empirical applications, and Section 6 concludes. Additional details are provided in the Supplementary Appendix.

2 American options and the early exercise premium

This section outlines key American option concepts relevant to the analysis. The estimator uses a cross-section of call and put options with the same maturity. Let t be the present time, T the expiration date, and S_v the underlying asset price at time v for $v \in [t, T]$. The equilibrium price of an American call option is given by $AmCall_t = \sup_{t \leq v \leq T} e^{-r(v-t)} E\left[(S_v - K)^+ | \mathcal{F}_t\right]$, where K is the strike price; $(X)^+ = \max(X, 0)$; r is the risk-free rate; and $\mathcal{F}_t$ is the information set at time t. The conditional expectation is taken with respect to the risk-neutral measure, and the supremum operator reflects that the option can be exercised at any time up to T.

The proposed SPD estimator is based on the following decomposition of $AmCall_t$:

$$AmCall_t = EuCall_t + EEC_t, \tag{1}$$

where $EuCall_t$ is the price of a European call option:

$$EuCall_t = e^{-r(T-t)} E\left[(S_T - K)^+ |\mathcal{F}_t\right], \tag{2}$$

and EEC_t is the early exercise premium (with δ representing the dividend rate):

$$EEC_t = \int_t^T e^{-r(v-t)} E\left[(\delta S_v - rK)\, 1_{(S_v \geq B_v)} |\mathcal{F}_t\right] dv. \tag{3}$$

This premium depends on the early exercise boundary B_t, where the option holder is indifferent between holding and exercising the option:

$$B_v - K = EuCall_v + EEC_v \quad \text{for any } v \in [t, T). \tag{4}$$

The left-hand side represents the revenue from exercising the option, and the right-hand side its continuing value, both evaluated at $S_v = B_v$. Kim and Yu (1996) and Detemple and Tian (2002) proved (1) and (3) for general diffusion models. For geometric Brownian motions, explicit expressions are available from Kim (1990), Jacka (1991), and Carr et al. (1992). For jump diffusions, (1) still holds but (3) requires modifications; see Gukhal (2001). This paper assumes there are no jumps when deriving the SPD estimator and then evaluates its performance under jumps using simulations. Similar expressions hold for put options; see Kim and Yu (1996). The framework here assumes fixed interest and dividend rates until maturity. Broadie et al. (2000) and Medvedev and Scaillet (2010) studied the theoretical implications of stochastic dividends or interest rates on American option pricing. Their empirical effects are not yet well documented.

Let $f_s^*(S_v) = f^*(S_v|\mathcal{F}_s)$, representing the SPD for the time-v distribution given the information available at time s. Once $f_s^*(S_v)$ is specified for $t \leq s \leq v \leq T$, the above expressions can be computed numerically or through simulations. Our estimation can be viewed as an inverse problem, where we infer the SPD from these expressions using observed option prices as input.

3 Proposed estimator

Our estimator combines a Gauss-Hermite approximation to the SPD, as proposed by Lu and Qu (2021), with a recursive equation for the early exercise premium. We first describe these two components and then present the estimation procedure.

3.1 Gauss-Hermite approximation and the early exercise premium

We use a transformation to stabilize the variance of the SPD as in Lu and Qu (2021). Let σ be the Black-Scholes implied volatility for the at-the-money call option, $\tau = T - t$, and define:

$$x = \frac{\log(S_T/S_t) - r\tau}{\sigma\sqrt{\tau}} \quad \text{and} \quad z = \frac{\log(K/S_t) - r\tau}{\sigma\sqrt{\tau}}. \tag{5}$$

Using $f_t(x)$ to represent the SPD of x, whose variance is approximately one by construction, the European call option in (2) can be written as

$$EuCall_t = \int_{-\infty}^{\infty} S_t \left[e^{\sqrt{\tau}\sigma x} - e^{\sqrt{\tau}\sigma z}\right]^+ f_t(x)dx. \tag{6}$$

Our estimation first recovers $f_t(x)$, and then we reverse the transformation in (5) to obtain the SPD for S_T, $f_t^*(x)$, as

$$f_t^*(S_T) = \frac{1}{\sigma\sqrt{\tau}S_T} f\left(\frac{\log(S_T/S_t) - r\tau}{\sigma\sqrt{\tau}}\right).$$

We approximate $f_t(x)$ in (6) using a Gauss-Hermite series expansion as in Lu and Qu (2021). This expansion is based on the Hermite functions $\{h_j\}$, a complete orthonormal system in $L^2(-\infty,\infty)$, defined as: $h_j(x) = [H_j(x)/(2^j j!\pi^{1/2})^{1/2}]e^{-x^2/2}$, where $\int_{-\infty}^{\infty} h_j^2(x)dx = 1$ for $j = 0, 1, 2, ...$; $\int_{-\infty}^{\infty} h_i(x)h_j(x)dx = 0$ for $i \neq j$; and $\{H_j(x)\}$ are physicist's Hermite polynomials: $H_j(x) = (-1)^j\, e^{x^2}(d^j/dx^j)e^{-x^2}$. Expanding $f_t(x)$ using $h_j(x)$ as basis functions, we have

$$f_t(x) = \sum_{j=0}^{\infty} \beta_j h_j(x) \text{ with } \beta_j = \int_{-\infty}^{\infty} f_t(x)h_j(x)dx. \tag{7}$$

Applying a truncation to (7), we obtain a Gauss-Hermite series approximation to $f_t(x)$:

$$f_t(x) \approx \sum_{j=0}^{J} \beta_j h_j(x). \tag{8}$$

Finally, after reversing the change-of-variables in (5), we obtain:

$$f_t^*(S_T) \approx \frac{1}{\sigma\sqrt{\tau}S_T}\sum_{j=0}^{J}\beta_j h_j\left(\frac{\log(S_T/S_t) - r\tau}{\sigma\sqrt{\tau}}\right). \tag{9}$$

We choose the Gauss-Hermite series for three reasons: (i) It expands around a standard normal density, with higher-order terms capturing deviations such as asymmetry and fat tails. Because the SPD is closely related to the normal density (e.g., when the underlying asset follows a geometric Brownian motion, the SPD in (6) is exactly N(0,1)), this expansion allows for a parsimonious approximation with just a few terms. (ii) The series converges under mild tail conditions, consistent with the SPD's tendency to exhibit fat tails. (iii) It spans the entire real line, capturing both the central part and the tails of the distribution. In contrast, compact-support polynomials, such as Chebyshev polynomials, cannot capture the tails effectively.

We now turn to the early exercise premium. The equation determining this premium is given by (c.f.(3)): $EEC_t = \int_t^T \int_0^\infty e^{-r(v-t)}\left(\delta S_v - rK\right) 1_{(S_v \geq B_v)} f_s^*(S_v) dS_v dv$, which involves the transition density $f_s^*(S_v)$. To compute this density, we use the same approximation as in (9):

$$f_s^*(S_v) \approx \frac{1}{\sigma\sqrt{v-s}S_v}\sum_{j=0}^{J}\beta_j h_j\left(\frac{\log(S_v/S_s) - r(v-s)}{\sigma\sqrt{v-s}}\right). \tag{10}$$

Given this approximation, we compute the early exercise boundary by numerically solving (4). This approximation is internally consistent because $f_s^*(S_v) \to f_t^*(S_T)$ as $s \to t$ and $v \to T$.

The transition density $f_s^*(S_v)$ is generally not identifiable from a single cross-section of options prices without additional assumptions. In (10), we assume it evolves with (s, v) via a deterministic transformation: its variance changes over time, while its shape remains constant. This is a strong assumption: it requires a process with independent, stationary increments, i.e., a Lévy process. It is thus crucial to test the method's performance when this assumption fails, such as when returns are driven by dependent state variables or exhibit dependent increments. We address this issue through simulations. That is, we generate data using five asset return models that collectively represent diverse markets, with parameter values calibrated to empirical estimates, to provide a realistic evaluation of the method; see Section 4 for details.

3.2 Estimation procedure

Let y_i and z_i $(i = 1, ..., n)$ denote the observed option prices and transformed strike prices at time t (c.f. (5)). The t index is omitted here and in subsequent discussions to simplify notation. The data are arranged so that the first n_c observations are call options, and the remaining $n - n_c$ observations are put options. Then, we have:

$$y_i = \begin{cases} EuCall_i + EEC_i + \varepsilon_i & \text{for } i = 1, ..., n_c, \\ EuPut_i + EEP_i + \varepsilon_i & \text{for } i = n_c + 1, ..., n. \end{cases}$$

In each equation, the first two terms represent the theoretical option price, and ε_i represent pricing errors. Define, for $j = 0, ..., J$:

$$x_{i,j} = \begin{cases} \int_{-\infty}^{\infty} S\left(e^{\sqrt{\tau}\sigma x} - e^{\sqrt{\tau}\sigma z_i}\right)^+ h_j(x)dx & \text{for } i = 1, ..., n_c, \\ \int_{-\infty}^{\infty} S\left(e^{\sqrt{\tau}\sigma z_i} - e^{\sqrt{\tau}\sigma x}\right)^+ h_j(x)dx & \text{for } i = n_c + 1, ..., n. \end{cases}$$

These $x_{i,j}$ terms will serve as the regressors in the regression. Let $x_i = (x_{i,0}, ..., x_{i,J})'$. The estimation procedure consists of three steps:

STEP 1. Obtain a preliminary estimate of the SPD: Assume $EEC_i = EEP_i = 0$ and solve

$$\min_{\beta \in \mathcal{H}_J} \sum_{i=1}^{n} \left(y_i - x_i'\beta\right)^2, \tag{11}$$

with

$$\mathcal{H}_J = \left\{\beta \in R^{J+1}\colon \inf_{x \in \mathbb{R}} \sum_{j=0}^{J} \beta_j h_j(x) \geq \eta\right\}, \tag{12}$$

where η is a small negative number accounting for the Gauss-Hermite approximation error. Let $(\hat{\beta}_0, ..., \hat{\beta}_J)$ be the estimate of β, and compute $\hat{f}(x) = \sum_{j=0}^{J} \hat{\beta}_j h_j(x)$.

STEP 2. Compute the early exercise boundary and early exercise premium using $\hat{f}(x)$: Let

$$\hat{f}_s^*(S_v) = \frac{1}{\sigma\sqrt{v-s}S_v} \sum_{j=0}^{J} \hat{\beta}_j h_j\left(\frac{\log(S_v/S_s) - r(v-s)}{\sigma\sqrt{v-s}}\right).$$

To determine the early exercise boundary of a call option with strike price K_i, solve numerically for B_v using: $\hat{B}_v - K_i = \widehat{EuCall}_v + \widehat{EEC}_v$ for any $v \in [t, T)$, where $\widehat{EuCall}_v$ and $\widehat{EEC}_v$ are the counterparts of $EuCall_v$ and EEC_v with $f_v^*(\cdot)$ and $B_v(\cdot)$ replaced by $\hat{f}_v^*(\cdot)$ and $\hat{B}_v(\cdot)$, respectively. The resulting estimate for the early exercise premium is

$$\widehat{EEC}_i = \int_t^T \int_{-\infty}^{\infty} e^{-r(v-t)} \left(\delta S_v - rK\right) 1_{(S_v \geq \hat{B}_v)} \hat{f}^*(S_v) dS_v dv.$$

Compute the early exercise premium for put options, denoted $\widehat{EEP}_i$, in a similar way.

STEP 3. Update the SPD estimate and the early exercise premium: First, use the early exercise premium from STEP 2 to re-estimate the SPD. Specifically, re-solve (11) after replacing y_i with $y_i - \widehat{EEC}_i$ for call options and $y_i - \widehat{EEP}_i$ for put options. Next, use this updated SPD estimate to recompute the early exercise premium as in STEP 2. Repeat this process until changes in the SPD estimate are small.

Remark 1 *STEP 1 produces an initial SPD estimate by treating American options as their European counterparts. STEP 2 calculates terms related to the early exercise feature based on this initial estimate. STEP 3 iteratively refines these estimates. This sequential approach breaks the computation into smaller parts, avoiding the complexity of a nonlinear optimization problem if all parameters were estimated in a single step.*

Remark 2 *By (7), the Gauss-Hermite approximation error equals* $f(x) - \sum_{j=0}^{J} \beta_j h_j(x) = \sum_{j=J+1}^{\infty} \beta_j h_j(x)$*, which can be negative for some* $x \in \mathbb{R}$*. Therefore, in* $\mathcal{H}_J$*, the parameter* η *should be slightly negative to account for the effect of the truncation. We suggest setting it to* η *=-1E-3. The optimization problem in STEP 2 is strictly convex because* $\mathcal{H}_J$ *is a convex set and the criterion function (11) is strictly convex. We use the* `solve.QP` *routine in R to implement this step. The parameter* J *controls the approximation error in (8). We suggest choosing* J *using ten-fold cross-validation over the set* $J = \{J^*, J^*+1, J^*+2\}$ *with* $J^* = ceiling(2*(n/log(n))^{0.2})$*. These recommendations follow Lu and Qu (2021). The estimator presented in this paper extends the methodology of Lu and Qu (2021) from European options to American options by incorporating STEPS 2 and 3 to account for the early exercise premium.*

4 Empirically calibrated simulations

In this section, we evaluate the performance of the proposed SPD estimator using five well-known parametric models as data-generating processes. These five models span diverse markets: equity index options, equity index futures options, volatility index options, and commodity options. We generate data using empirically calibrated parameter values. A summary of these data-generating processes is provided below, with more details available in the appendix.

Heston's stochastic volatility (SV) model. This is a benchmark model for pricing equity and equity index options. The model specifies the risk-neutral dynamics of the spot price of the underlying asset as

$$dS_t = (r - \delta)S_t dt + \sqrt{V_t} S_t dW_t,$$
$$dV_t = \kappa(\theta - V_t)dt + \sigma\sqrt{V_t} dU_t,$$

where r represents the risk-free rate, δ represents the dividend rate, W_t and U_t are two Brownian motions with a correlation coefficient ρ. The parameter θ determines the long-run variance level, κ affects the speed of mean-reversion, and σ is the volatility-of-volatility parameter. For simulations, we use the parameters from the SV panel of Table 1 of Lu and Qu (2021), estimated using S&P500 index options from the period 2013.06–2013.12. The simulated sample consists of 79 call options and 79 put options; therefore, the sample size is $n = 158$.

Two-factor SV model. As a generalization of the basic SV model, this model allows two factors in the volatility process ($i = 1, 2$):

$$dS_t/S_t = rdt + \sqrt{V_{1,t}} dW_{1,t} + \sqrt{V_{2,t}} dW_{2,t},$$
$$dV_{i,t} = (\alpha_i - \beta_i V_{i,t})dt + \sigma_i\sqrt{V_{i,t}} dU_{i,t},$$

with $Cov(dW_{i,t}, dU_{i,t}) = \rho_i dt$, and $Cov(dW_{1,t}, dW_{2,t}) = Cov(dU_{1,t}, dU_{2,t}) = 0$. For simulations, we use parameter values from Bates (2000, p.203), estimated using S&P500 futures options. The simulated sample consists of 111 call and 111 put options.

DMR model. This model is mainly used for variance swaps, currency options, and interest rates, and it appeared in Bates (2012), Mencia and Sentana (2013), and Xiu (2014). Our DGP is the same as that in Mencia and Sentana (2013):

$$dV_t = \beta(\theta_t - V_t)dt + \sigma\sqrt{V_t}dW_t,$$
$$d\theta_t = \xi(\alpha - \theta_t)dt + \kappa\sqrt{\theta_t}dU_t,$$

where V_t is a variance instrument, and W and U are two independent Wiener processes. The parameter values are taken from Table 4 of Mencia and Sentana (2013) for an empirical analysis of VIX derivative valuation models. The simulated sample consists of 51 call and 51 put options.

CEV model. The constant elasticity of variance (CEV) model, introduced by Cox (1996), is a generalization of the Geometric Brownian Motion, allowing the conditional variance of asset returns to depend on the price level. This model has been applied in various contexts, such as modeling short-term interest rates and pricing commodity options. We use the following DGP:

$$dV_t/V_t = (r - \delta)dt + \sigma V_t^{\beta} dW_t.$$

The parameter values are taken from Geman and Shih (2008), based on crude oil over the period 01/01/2000 to 12/11/2007, and were also used in Carlos Dias and Pedro Vidal Nunes (2011). The simulated sample consists of 57 call and 57 put options.

SVCJ model. This is a stochastic volatility model with contemporaneous jumps in return and volatility, proposed by Duffie, Pan, and Singleton (2000):

$$dS_t/S_t = rdt + \sqrt{V_t}dW_t + (e^{Z_t^s} - 1)dN_t - \lambda\mu dt$$
$$dV_t = \kappa(\theta - V_t)dt + \sigma\sqrt{V_t}dU_t + Z_t^v dN_t,$$

where the definitions of the variables are the same as in the SV case, $N_t \sim \text{Poi}(\lambda)$ is a Poisson counting process with a constant intensity λ; Z_t^s denotes jump in return with $Z_t^s \sim \mathcal{N}(\mu_s, \sigma_s^2)$; and Z_t^v denotes jump in volatility which follows an exponential distribution: $Z_t^v \sim \text{Exp}(\mu_v)$. θ

determines the long-run variance level, κ affects the speed of mean reversion, σ is the volatility-of-volatility parameter, and $-\lambda\mu$, with $\mu = \exp(\mu_s + \sigma_s^2/2) - 1$, compensates for the instantaneous change in the expected return due to the presence of Z_t^s. This DGP, with parameter values from the SVCJ panel of Table 1 in Lu and Qu (2021), is included to assess estimation accuracy when jumps are present. The simulated sample consists of 79 call and 79 put options.

We divide the analysis into two parts. First, we evaluate the methods when the pricing relationship is exact, meaning there is no noise in option prices. This setup allows us to assess the adequacy of the Gauss-Hermite and early exercise premium approximations without the interference of estimation uncertainty. It also enables us to quantify the estimation bias caused by disregarding the early exercise feature (i.e., treating American options as European options). In the second part, we introduce noise into the option prices and evaluate the finite-sample performance of the proposed methods. The truncation order of the Hermite approximation is determined via ten-fold cross-validation over the set $\{J^*, J^*+1, J^*+2\}$ with $J^* = ceiling(2 * (n/log(n))^{0.2})$. Option prices are generated using Longstaff and Schwartz's (2001) method, with maturity set to one year; results for a six-month horizon are included in the appendix.

4.1 Adequacy of approximations

We present the results in five figures: Figure 1 for the SV model and Appendix Figures A.1-A.4 for the remaining four models. Each figure contains four panels. Panel (a) displays the SPD estimate using European option prices, representing the ideal situation where the unknown early exercise premium is replaced by its true value. Panel (b) displays the conventional approach, which treats American options as European options and leads to biased estimates. Panel (c) presents the proposed estimator, and panel (d) displays the estimated and true early exercise premiums. The red solid curve represents the true value, and the black dashed line the estimate. The estimates in panels (a) and (b) are obtained using the sieve method of Lu and Qu (2021).

Figure 1 shows that large estimation biases occur when the early exercise feature is ignored

Figure 1: SPD and EEP estimates for the SV model

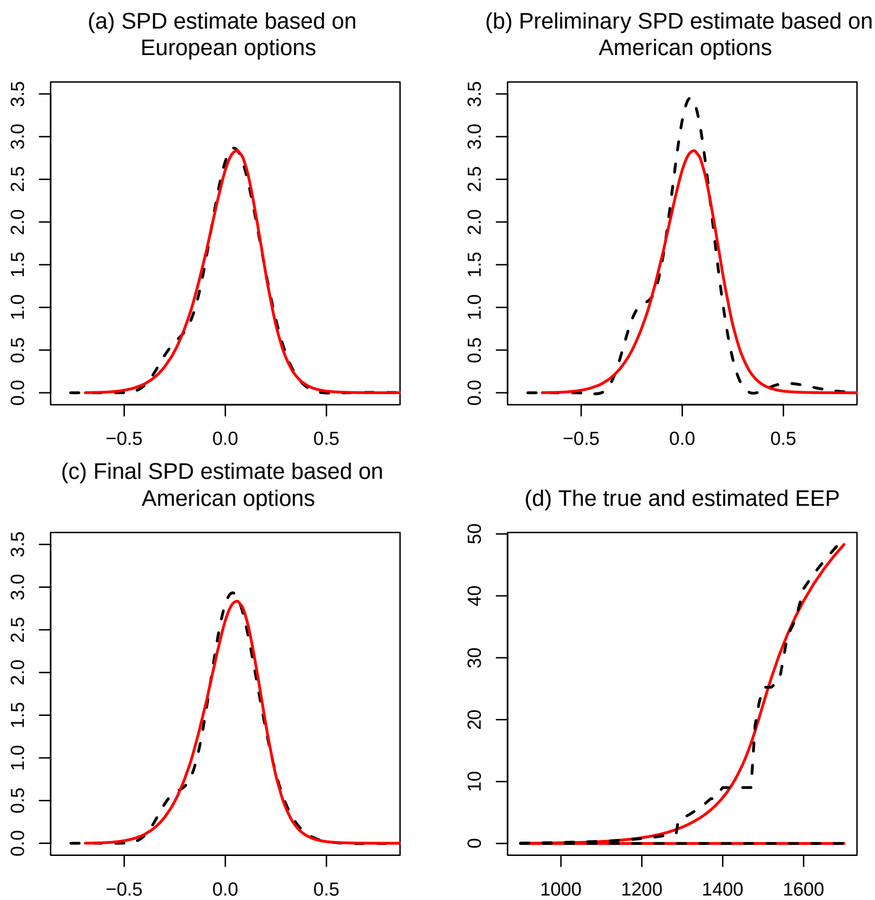

Note. SPD: state price density for the return. EEP: early exercise premium. Horizon: 1-year. Solid curve: true value. Dashed line: estimates. In (d), the increasing part is the put option EEP. See Appendix for more details about the DGP.

(Panel b of Figure 1). It also shows that accounting for the early exercise premium using the proposed methods improves the estimate substantially (Panel c). The resulting estimate is close to the infeasible counterpart (Panel a). Although the estimated early exercise premium sometimes deviates from the true value for in-the-money put options, there is no visible detrimental effect on the SPD estimation. This suggests that for estimating the SPD, an approximate value of the early exercise premium is sufficient, rather than its exact value.

Figures A.1-A.4 for the remaining four models lead to similar conclusions as Figure 1.

The proposed methods perform well in the SVCJ model case, even though the early exercise boundary formula does not explicitly account for jumps. Additionally, Figures A.5-A.9 provide evidence that incorporating the early exercise premium can be important even at the six-month horizon: for the SV, two-factor SV, and SVCJ models, neglecting the early exercise premium results in significant biases which the proposed methods are able to reduce effectively.

4.2 Finite sample performance

We now introduce noise to option prices. We generate option prices as in Section 4.1 and add independent noise uniformly distributed between -10% and 10% of the price level. We cap the noise by an upper bound: for Heston's SV, the two-factor SV, and the SVCJ models, we set it to 5 or 10 dollars. For the DMR and CEV models, we set it to 50 cents or 1 dollar because the option prices are lower (with maximum option prices approximately 149 and 77 in these two cases, respectively). This simulation design follows Lu and Qu (2021).

We compare with Melick and Thomas's (1997) and Tian's (2011) methods. Melick and Thomas (1997) specified the SPD as a mixture of three lognormals (the MLN estimator):

$$f_t^{MLN}(S_T) = \sum_{i=1}^{3} \frac{\pi_i}{\sqrt{2\pi}\sigma_i S_T} \exp\left[-\frac{1}{2}\left(\frac{\log(S_T) - \mu_i}{\sigma_i}\right)^2\right],$$

where $\sum_{i=1}^{3} \pi_i = 1$, and $\pi_i > 0$ for $i = 1, 2, 3$. To address the early exercise premium, Melick and Thomas (1997) derived bounds of American option prices relative to their European counterparts and estimated the nine parameters $(\pi_i, \mu_i, \sigma_i), i = 1, 2, 3$, by minimizing the sum of squared option pricing errors. Tian's (2011) method is based on estimating a binomial tree (hereafter, the iIB estimator). Starting with an initial value for the SPD, the method calculates the implied early exercise premium and subtracts this value from the American option prices to estimate the European option prices. It then fits the resulting European option prices to a binomial tree. Tian (2011) did not specify the number of iterations in the paper but noted that convergence is fast. We use four iterations, the same as our proposed method.

Table 1: Bias and MISE of Estimators

Method	Error bound: \$5		Error bound: \$10	
A. SV model				
	$Bias^2$	MISE	$Bias^2$	MISE
Proposed	**0.0079**	**0.0132**	**0.0077**	**0.0179**
*i*IB	0.0502	0.0503	0.0502	0.0503
MLN	0.0127	0.0287	0.0134	0.0325
MMT	0.0185	0.0213	0.0164	0.0215

Method	Error bound: \$5		Error bound: \$10	
B. TFSV model				
	$Bias^2$	MISE	$Bias^2$	MISE
Proposed	**0.0032**	**0.0129**	**0.0034**	**0.0166**
*i*IB	0.0238	0.0239	0.0238	0.0239
MLN	0.0357	0.0440	0.0357	0.0445
MMT	0.0360	0.0376	0.0362	0.0382

Method	Error bound: \$0.5		Error bound: \$1	
C. DMR model				
	$Bias^2$	MISE	$Bias^2$	MISE
Proposed	0.0061	**0.0107**	0.0070	0.0138
*i*IB	0.0110	0.0112	0.0110	**0.0113**
MLN	0.0137	0.0381	0.0121	0.0420
MMT	**0.0044**	0.0120	**0.0045**	0.0168

Method	Error bound: \$0.5		Error bound: \$1	
D. CEV model				
	$Bias^2$	MISE	$Bias^2$	MISE
Proposed	**0.0008**	**0.0039**	**0.0003**	0.0066
*i*IB	0.0051	0.0052	0.0052	**0.0052**
MLN	0.0142	0.0200	0.0134	0.0204
MMT	0.0176	0.0261	0.0144	0.0332

Method	Error bound: \$5		Error bound: \$10	
E. SVCJ model				
	$Bias^2$	MISE	$Bias^2$	MISE
Proposed	**0.0094**	**0.0139**	**0.0083**	**0.0176**
*i*IB	0.0531	0.0535	0.0521	0.0535
MLN	0.0165	0.0325	0.0168	0.0366
MMT	0.0176	0.0207	0.0161	0.0213

Note. $Bias^2$: the squared bias; MISE: the mean integrated squared error. Averages over 5000 replications are reported, with the lowest value in each case highlighted in bold. In A-E, the rows correspond to the proposed estimator (row 1), Tian's (2011) *i*IB estimator (row 2), Melick and Thomas's (1997) MLN estimator (row 3), and the estimator combining the sieve method with Melick and Thomas's (1997) approach for the early exercise premium (row 4).

We also compare with a new estimator that serves as a middle ground between Melick and Thomas's and our estimator. It combines Lu and Qu's (2021) sieve method for European-

SPD estimation with Melick and Thomas's approach to handling the early exercise premium. This helps explain performance differences between the proposed and Melick and Thomas's estimators, whether due to the approximation framework (sieve vs. mixture) or the treatment of the early exercise premium. We call it the Modified Melick-Thomas (MMT) estimator.

Table 1 presents the mean squared biases and mean squared errors (MISE) for ten cases (five models, each at two noise levels). The lowest bias or MISE in each case is highlighted in bold. Compared to Tian's (2011) and Melick and Thomas's (1997) estimators, the proposed estimator achieves smaller biases in all ten cases and lower MISE in eight cases. In seven of these, the MISE is reduced by at least 25% relative to the second-best method. For the remaining two cases (DMR and CEV with a noise bound of $1), the proposed method ranks second, with MISE values slightly higher than the best method. The proposed estimator produces smaller biases than the modified Melick-Thomas estimator in eight cases and smaller MISE in all ten cases. This shows that the new approach for estimating the early exercise premium plays a critical role in driving the performance of the proposed estimator.

The MISE of the *i*IB method changes only slightly when the error bound is doubled. This is because the method, based on binomial trees, is essentially parametric, with estimation bias often dominating variance. As the bias is largely unaffected by noise increases and the variance is small, the MISE shows only slight variation across noise levels.

5 Empirical applications

This section presents two empirical applications: one to SPY options (where SPY is an ETF designed to track the S&P 500 index) and the other to a set of options on individual stocks.

5.1 SPY options

We conduct this empirical application with two goals: to evaluate whether the method can recover the SPD and early exercise premium and to test if the recovered SPD can predict future asset returns at different horizons.

The first goal poses a challenge because most financial assets do not have European and American options simultaneously, making it difficult to measure the early exercise premium. However, we have identified a pair of assets that offer valuable insights: the S&P500 index (SPX), and an ETF called SPY, which tracks the SPX. These two assets co-move closely, as shown in Appendix Figure A.10, which displays these two series from 01/01/2007 to 02/28/2023. Further details on these two series are provided in Supplementary Appendix Section A2. The S&P500 index has European-style options, while the SPY options are American-style. Given the strong correlation between the two, SPY options can be viewed as approximately equivalent to SPX options, with price differences primarily reflecting the early exercise premium. This enables us to use the SPD computed from SPX options as a benchmark to evaluate the accuracy of our method in recovering the SPD from American-style SPY options.

We collect daily observations from OptionMetrics and process the data as follows: (1) Remove all strikes with zero open interest to exclude outdated information. (2) Retain only option contracts that expire on the third Friday of any month. (3) Keep contracts with maturities of approximately 1, 3, 6, and 12 months, or equivalently, with τ = 30, 91, 182, or 365 days. Specifically, for τ = 30 or 91 days, retain contracts expiring within [τ-2, τ+2] days, and for τ = 182 or 365 days, retain those within [τ-5, τ+5] days. This window ensures that actual return horizons do not deviate significantly from their targets. If two contracts are equidistant from maturity (e.g., 28 days and 32 days when τ = 30), select the contract with more strikes. (4) For each contract, exclude trading days with fewer than 40 available strikes to ensure sufficient observations for estimation. The resulting sample sizes are given in Table 2.

Table 2: Sample sizes for different maturities

	$\tau = 30$	$\tau = 91$	$\tau = 182$	$\tau = 365$
SPX	192	182	90	68
SPY	192	164	89	73

5.1.1 SPDs implied by SPX or SPY options

We compare SPDs estimated from SPX with those from SPY options. We begin with a close examination of a specific date and then report estimates for all available days in this sample period. The date chosen is 02/17/2023, the most recent Friday available in the data at the time of writing this paper. On that date, the short-term interest rate was at 5.6%, reflecting the Fed's efforts to raise rates to tame inflation after COVID. The option maturity is 336 days.

Panel (a) of Figure 2 shows three SPD estimates: the solid black curve is based on SPX options, the solid red curve uses SPY ETF options with the proposed method, and the dashed blue curve uses SPY ETF options while ignoring the early exercise feature. The results show that the proposed method produces an SPD close to the one from European options, while ignoring the early exercise feature introduces significant bias. The integrated mean squared error relative to the European-option-based estimate (solid black curve) is 4.3E-2 when the early exercise feature is ignored, compared to 2.5E-3 when it is accounted for.

Panel (b) displays the estimated early exercise premiums (the solid curve) and their true values calculated as differences between SPY and SPX option prices (circles). The estimates adequately capture the put option early exercise premiums and correctly indicate that the call premiums are nearly zero. In Panel (c), the actual SPY ETF option values (circles) are plotted alongside the fitted values produced by the proposed method (solid line). The fitted values are close to the actual option values across the full range of strike prices.

Next, we report estimates for all available days in this period by plotting their 0.1, 0.25, 0.5, 0.75, and 0.9 quantiles alongside actual realized future returns. Results for the monthly maturity case are presented in Figure 3, while other maturities are shown in Supplementary Appendix Figures A.13-A.15. Figure 3 confirms that the SPDs implied by SPX and SPY options are close to each other at the 1-month horizon. The root mean squared differences between their values on common transaction dates are 0.010, 0.004, 0.003, 0.003, and 0.004 for

Figure 2: SPD and EEP estimates for 02/17/2023

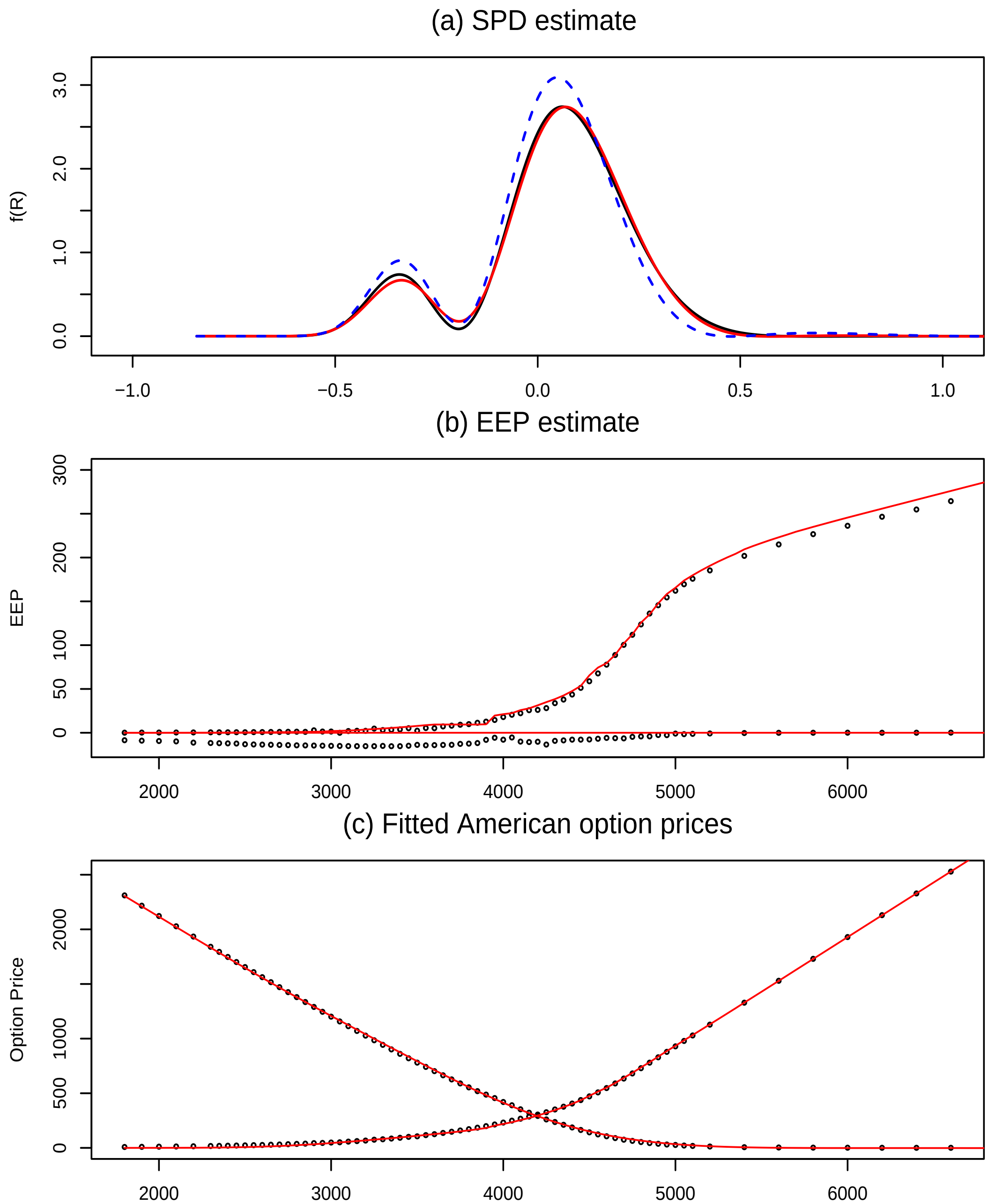

Note. Panel (a): the solid black curve is based on SPX options; the solid red curve uses SPY ETF options with the proposed method; and the dashed blue curve uses SPY ETF options while ignoring the early exercise premium. Panel (b): the red curves show the estimated early exercise premiums, and the black circles represent the actual EEP values, calculated as differences between SPY and SPX option prices. Panel (c): the red solid curves represent the fitted option values produced by the proposed method and the black circles show the actual SPY option prices. The expiration is 336 days, with SPX and SPY spot prices of 4079.1 and 4072.6, respectively.

$\tau = 0.1$, 0.25, 0.5, 0.75, and 0.9, respectively. Both distributions are left-skewed, with the 10th percentile showing more extreme negative values than the 90th percentile shows positive values, particularly during periods of market stress such as the recent financial crisis and the COVID pandemic. The results also reveal sharp fluctuations in the tails, while the median stays stable. This suggests that the tails may contain more predictive information about future returns than

Figure 3: SPD estimates for $\tau = 30$ days

(a) SPY ETF implied densities

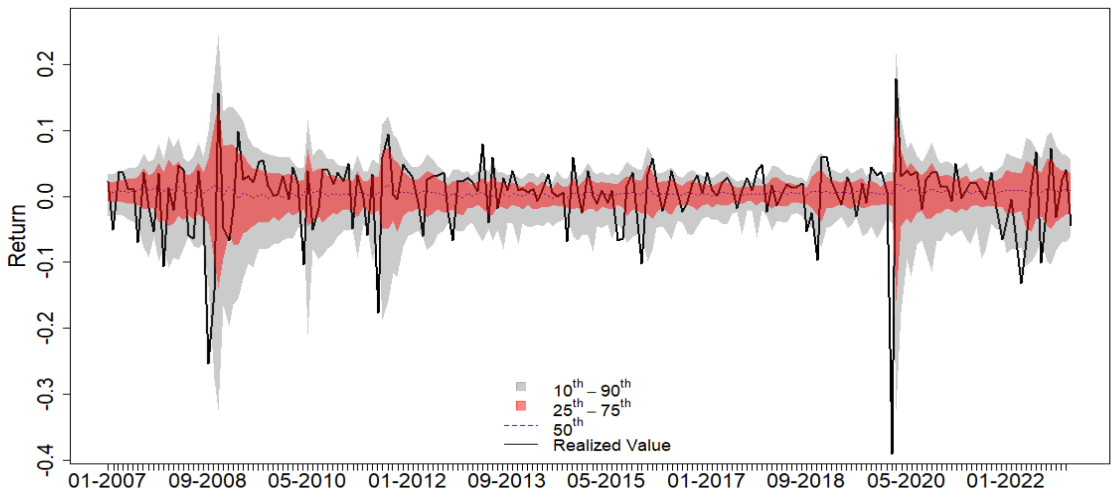

(b) SPX implied densities

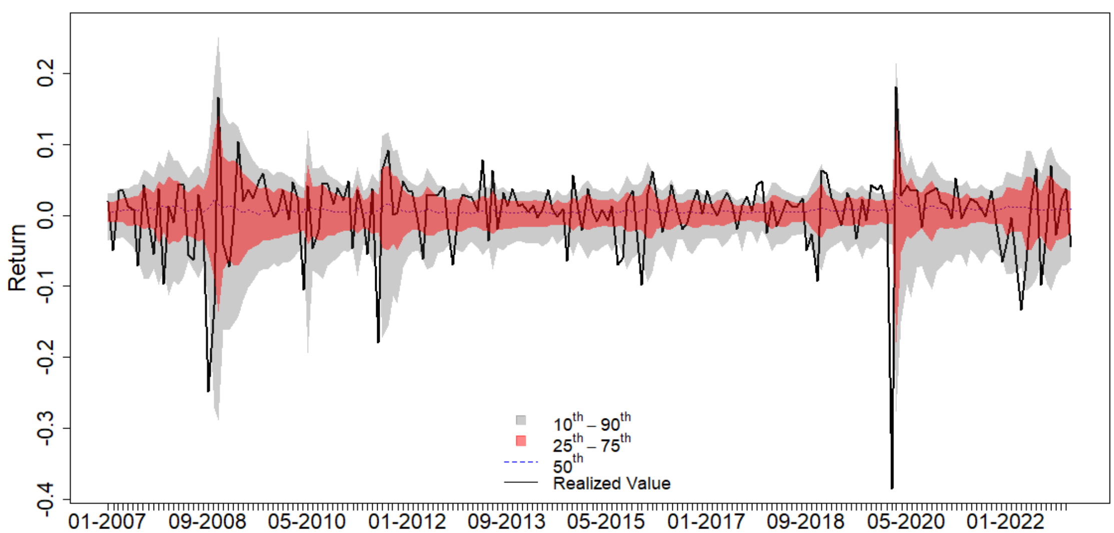

the center. These findings are consistent with Lu and Qu (2021), who studied S&P 500 index options for 2007-2016. Figure A.15 displays the SPD estimates for the annual horizon. As in the monthly case, the densities implied by SPX and SPY resemble each other. The root mean squared differences on common transaction dates are 0.018, 0.018, 0.008, 0.006, and 0.010 for $\tau = 0.1$, 0.25, 0.5, 0.75, and 0.9, respectively. The leftward skewness is more pronounced than in the monthly case, as shown by the 10th and 90th percentiles. Appendix Figures A.13 and A.14 present results for 3- and 6-month horizons, respectively, which support the findings from the monthly and annual cases. Next, we turn to predictive regressions.

5.1.2 Predictive power of the state price density

Each SPD represents a distribution, which enables the use of measures such as the mean, variance, or quantiles to predict future returns. Motivated by the comovements between SPD quantiles and future returns observed in Figures 3 and A.15, we focus on quantiles as predictors. Lu and Qu (2021) conducted a similar analysis for S&P 500 index options at the monthly horizon over 2007 to 2016. Here, we extend their analysis to American options, consider longer horizons of up to one year, and incorporate the COVID into the study.

We consider both mean and quantile regressions. In all cases, the dependent variable is the return on the SPY ETF. For the mean regression, a quantile of the SPD is used to predict the future return. We run nine regressions, each using a decile of the SPD as the predictor. For the quantile regression, a specific quantile, such as the 10th percentile of the SPD, is used to predict the same percentile of the future return distribution. These two regressions complement each other, as they allow us to assess the predictive power for both the central tendency and the shape of the return distribution. To ensure all conditioning information is available for prediction, the SPD is computed using the dividend rate from the previous year. We also conducted regressions using SPX returns and SPX options, and the results were similar.

We consider three sample periods to evaluate how predictability might change in response

Table 3: Predictive regression using a quantile of the SPD as predictor (τ=30 days)

Quantile	0.10	0.20	0.30	0.40	0.50	0.60	0.70	0.80	0.90
				(a) 06/2009-02/2020					
Estimate	-0.42	-0.84	-1.32	-1.85	1.49	1.68	1.16	0.86	0.62
s.e.	0.12	0.31	0.57	1.08	1.09	0.52	0.34	0.24	0.17
t-value	-3.54	-2.69	-2.34	-1.72	1.37	3.25	3.41	3.65	3.69
p-value	**0.00**	**0.01**	**0.02**	**0.09**	0.17	**0.00**	**0.00**	**0.00**	**0.00**
R^2	0.05	0.04	0.03	0.02	0.01	0.03	0.04	0.04	0.04
				(b) 06/2009-02/2023					
Estimate	-0.46	-0.79	-1.52	-2.96	2.09	1.81	1.21	0.89	0.64
s.e.	0.12	0.15	0.44	1.33	1.21	0.67	0.39	0.26	0.19
t-value	-3.98	-5.26	-3.43	-2.22	1.73	2.72	3.10	3.40	3.46
p-value	**0.00**	**0.00**	**0.00**	**0.03**	**0.09**	**0.01**	**0.00**	**0.00**	**0.00**
R^2	0.09	0.09	0.08	0.06	0.02	0.06	0.07	0.08	0.08
				(c) 01/2007-02/2023					
Estimate	-0.21	-0.43	-0.75	-1.63	0.50	0.79	0.57	0.41	0.30
s.e.	0.17	0.24	0.45	0.86	1.42	0.80	0.47	0.33	0.23
t-value	-1.20	-1.81	-1.69	-1.90	0.36	0.98	1.20	1.27	1.32
p-value	0.23	**0.07**	**0.09**	**0.06**	0.72	0.33	0.23	0.21	0.19
R^2	0.03	0.04	0.03	0.03	0.00	0.01	0.02	0.02	0.03

Note. Dependent variable: return on SPY. Independent variable: a quantile of the SPD implied by SPY options. An intercept is always included. The standard errors account for heteroscedasticity and autocorrelation. Estimates significant at the 10% level are in bold.

to extreme market conditions: a benchmark sample from 2009.6 to 2020.2, an extended sample including the COVID pandemic (2009.6-2023.2), and a further extended sample including the 2008 financial crisis (2007.1-2023.2). We consider four different maturities for each sample period as in the previous subsection: $\tau = 30$, 91, 182, and 365 days.

Tables 3-6 present results from the mean regressions for different predictive horizons. Each column in the tables corresponds to a separate least-squares regression. For example, the first column of Table 3 shows the regression of the monthly return on the 10th percentile of the lagged SPD. P-values significant at the 10% level are highlighted in bold.

Table 4: Predictive regression using a quantile of the SPD as predictor (τ=91 days)

Quantile	0.10	0.20	0.30	0.40	0.50	0.60	0.70	0.80	0.90
					(a) 06/2009-02/2020				
Estimate	-0.45	-1.24	-2.25	-4.00	-0.28	1.70	1.40	1.03	0.77
s.e.	0.20	0.40	0.74	1.76	1.85	0.76	0.48	0.35	0.26
t-value	-2.30	-3.12	-3.04	-2.28	-0.15	2.23	2.91	2.93	2.92
p-value	**0.02**	**0.00**	**0.00**	**0.02**	0.88	**0.03**	**0.00**	**0.00**	**0.00**
R^2	0.09	0.10	0.10	0.08	0.00	0.03	0.06	0.06	0.07
					(b) 06/2009-02/2023				
Estimate	-0.49	-1.34	-2.64	-5.05	1.33	1.86	1.43	1.06	0.80
s.e.	0.21	0.47	0.93	1.80	2.20	1.10	0.67	0.45	0.32
t-value	-2.31	-2.86	-2.83	-2.81	0.60	1.70	2.15	2.36	2.49
p-value	**0.02**	**0.00**	**0.01**	**0.01**	0.55	**0.09**	**0.03**	**0.02**	**0.01**
R^2	0.13	0.15	0.15	0.11	0.01	0.07	0.10	0.11	0.12
					(c) 01/2007-02/2023				
Estimate	-0.39	-0.69	-1.42	-2.99	-0.49	0.81	0.72	0.55	0.42
s.e.	0.23	0.56	0.93	1.55	2.38	1.33	0.83	0.57	0.40
t-value	-1.68	-1.24	-1.53	-1.93	-0.21	0.61	0.86	0.98	1.04
p-value	**0.10**	0.22	0.13	**0.06**	0.84	0.55	0.39	0.33	0.30
R^2	0.06	0.04	0.05	0.04	0.00	0.01	0.02	0.03	0.03

Note. Dependent variable: return on SPY. Independent variable: a quantile of the SPY-implied SPD. An intercept is always included. The standard errors account for heteroscedasticity and autocorrelation. Estimates significant at the 10% level are in bold.

Consider the benchmark sample period corresponding to panels (a) in these tables. The p-values consistently indicate a significant predictive relationship at the 10% level, except for quantiles near the center of the distribution. The coefficient estimates are negative at lower quantiles and positive at upper quantiles. The regression R-squares are low, as expected, but tend to increase with the horizon: for the monthly horizon, they range from 1% to 5%, while for the annual horizon, they range from 1% to 13%. These results point to a significant predictive relationship between the SPD and future returns during this period, with the signs of the coefficients consistent with a risk-expected return trade-off interpretation.

Table 5: Predictive regression using a quantile of the SPD as predictor (τ=182 days)

Quantile	0.10	0.20	0.30	0.40	0.50	0.60	0.70	0.80	0.90
(a) 6/2009-2/2020									
Estimate	-0.30	-0.99	-1.86	-3.02	-1.29	1.46	1.37	0.99	0.70
s.e.	0.21	0.35	0.62	1.18	2.53	1.52	0.79	0.50	0.33
t-value	-1.42	-2.82	-3.01	-2.55	-0.51	0.96	1.74	1.97	2.11
p-value	0.16	**0.01**	**0.00**	**0.01**	0.61	0.34	**0.09**	**0.05**	**0.04**
R^2	0.04	0.13	0.14	0.11	0.01	0.03	0.06	0.07	0.08
(b) 6/2009-2/2023									
Estimate	-0.58	-1.50	-3.04	-4.42	0.81	2.12	1.67	1.25	0.91
s.e.	0.29	0.39	1.07	1.64	2.08	1.53	0.96	0.65	0.42
t-value	-1.99	-3.87	-2.85	-2.69	0.39	1.39	1.75	1.93	2.16
p-value	**0.05**	**0.00**	**0.01**	**0.01**	0.70	0.17	**0.08**	**0.06**	**0.03**
R^2	0.15	0.25	0.23	0.14	0.00	0.09	0.13	0.15	0.17
(c) 1/2007-2/2023									
Estimate	-0.55	-1.01	-2.02	-4.14	-2.63	0.39	0.73	0.65	0.52
s.e.	0.27	0.41	0.67	0.78	2.89	1.83	1.04	0.65	0.42
t-value	-2.08	-2.44	-3.00	-5.30	-0.91	0.21	0.71	1.01	1.22
p-value	**0.04**	**0.02**	**0.00**	**0.00**	0.36	0.83	0.48	0.32	0.23
R^2	0.10	0.11	0.12	0.15	0.04	0.00	0.02	0.03	0.05

Note. Dependent variable: return on SPY. Independent variable: a quantile of the SPY-implied SPD. An intercept is always included. The standard errors account for heteroscedasticity and autocorrelation. Estimates significant at the 10% level are in bold.

Next, consider panels (b) in these tables, which incorporate the COVID period. For the 1- to 6-month horizons, the results are similar to those from the 2009–2020 sample, consistently showing a significant predictive relationship. For the annual horizon, the point estimates remain comparable to 2009–2020, but only quantiles 0.2, 0.3, and 0.4 are statistically significant. Thus, evidence of predictability is weaker in the annual horizon case for this sample.

Finally, consider panels (c), which include the 2008 financial crisis. The results show that quantiles above the median are insignificant, while those below the median vary in significance. The predictability is strongest at the semi-annual and annual horizons, where all lower quantiles

Table 6: Predictive regression using a quantile of the SPD as predictor (τ=365 days)

Quantile	0.10	0.20	0.30	0.40	0.50	0.60	0.70	0.80	0.90
				(a) 06/2009-02/2020					
Estimate	-0.49	-0.65	-1.23	-1.39	-0.96	0.58	1.41	1.11	0.77
s.e.	0.21	0.23	0.57	0.79	1.11	1.10	0.68	0.48	0.34
t-value	-2.32	-2.86	-2.14	-1.77	-0.87	0.52	2.08	2.33	2.30
p-value	**0.02**	**0.01**	**0.04**	**0.08**	0.39	0.60	**0.04**	**0.02**	**0.03**
R^2	0.08	0.13	0.11	0.07	0.02	0.01	0.06	0.08	0.09
				(b) 06/2009-02/2023					
Estimate	-0.52	-0.98	-2.02	-2.41	-1.10	0.54	1.06	0.88	0.67
s.e.	0.38	0.18	0.69	0.98	1.19	1.69	1.27	0.85	0.52
t-value	-1.36	-5.59	-2.93	-2.45	-0.92	0.32	0.83	1.04	1.28
p-value	0.18	**0.00**	**0.00**	**0.02**	0.36	0.75	0.41	0.30	0.20
R^2	0.08	0.28	0.17	0.11	0.02	0.01	0.05	0.07	0.09
				(c) 01/2007-02/2023					
Estimate	-0.66	-0.95	-1.90	-3.06	-3.15	-0.92	0.40	0.54	0.49
s.e.	0.25	0.14	0.37	0.76	1.38	1.62	0.99	0.58	0.34
t-value	-2.65	-7.02	-5.12	-4.01	-2.29	-0.57	0.40	0.93	1.46
p-value	**0.01**	**0.00**	**0.00**	**0.00**	**0.03**	0.57	0.69	0.35	0.15
R^2	0.13	0.24	0.19	0.19	0.14	0.02	0.01	0.03	0.05

Note. Dependent variable: return on SPY. Independent variable: a quantile of the SPY-implied SPD. An intercept is always included. The standard errors account for heteroscedasticity and autocorrelation. The estimates significant at the 10% level are in bold.

are significant, and weakest at the quarterly horizon, with only the 10th and 40th percentiles significant. The financial crisis appears to have disrupted the predictive relationship, and lower quantiles are more relevant predictors than upper quantiles for this extended sample period.

In summary, these regressions suggest the existence of a predictive relationship between quantiles of the SPD and realized returns, especially when the 2008 financial crisis is not included in the sample. Lower quantiles show stronger predictive power than upper quantiles. Intuitively, a downward shift in the lower quantiles of the SPD is often triggered by negative market events (e.g., the 2008 financial crisis or the onset of COVID). Over the past 20 years, markets have generally recovered well from large declines, making such shifts in lower quantiles investment opportunities that yielded higher returns, especially over longer horizons.

In the tables, the standard errors for the t-tests are computed using the `sandwich` package in R, with the quadratic spectral kernel and the bandwidth selection method of Andrews (1991). We also implement two recommended methods for HAR inference from Lazarus et al. (2018) to assess robustness. See Appendix Tables A.1 and A.2 and their footnotes for details. The patterns of statistical significance are similar to those reported above. The test loses significance in only a few cases, and the conclusions stated in the previous paragraph remain the same.

We next turn to predictive quantile regressions, reported in Appendix Tables A.3-A.6. The results reveal clear patterns for the 1- to 6-month horizons. For quantiles above the median, the estimates are statistically significant with only two exceptions (see panels (a) and (c) in Table A.5), regardless of whether the COVID period or the 2008 financial crisis is included in the sample. For quantiles below the median, the estimates are insignificant in most cases. Lu and Qu (2021) observed a similar pattern for S&P500 options at a 1-month horizon. Our findings extend their result to SPY options and longer horizons up to six months. Finally, for the annual horizon, the results are mixed: for quantiles above the median, half of the estimates are significant, not leading to clear conclusions. We evaluate these findings using the methods of Fan and Lee (2019) for the monthly horizon and the approach of Gungor and Luger (2021) for all horizons, and the conclusions remain unchanged. See Tables A.7 and A.9-A.11 for details.

These regressions show that the lower quantiles of the SPD can predict future returns on average but may not predict the corresponding quantile of the return distribution. A decline in lower quantiles is typically triggered by negative events. Since markets have generally recovered well from significant declines, actual outcomes often exceeded initial pessimistic expectations. In other words, the lower quantiles of the SPD captured a fear or risk premium that was accompanied by higher, rather than lower, subsequent returns. As a result, these quantiles do not closely correlate with the lower quantiles of the actual return distribution.

5.2 Stock options

We estimate SPDs implied by individual stock options and evaluate their predictive power for future returns. The data are obtained from OptionMetrics for the period 01/1996 to 12/2021. We first identify all stocks with traded options during this period and then apply the following filters to process the options data: (1) Following Goyal and Saretto (2009), exclude observations where the mid-prices violate the arbitrage bounds, the ask price is lower than the bid price, the bid price is equal to zero, or the bid–ask spread is lower than the minimum tick size. (2) Remove all strikes with zero open interest. (3) As in our previous application, for each stock, select only the contracts that expire on the third Friday of any month with maturities of approximately 30, 91, 182, or 365 days (1, 3, 6 or 12 months). (4) Finally, for any contract, exclude trading days with fewer than 20 available strikes to ensure liquidity. The resulting dataset represents an unbalanced monthly panel, summarized in Table 7. We also consider a subsample from 06/2009 to 02/2020, excluding the 2008 crisis and COVID pandemic, to test result sensitivity.

Table 7: Stock options data: 1996–2021

Days to maturity	30	91	182	365
No. of firms	193	117	149	100
Total no. of contracts	31,794	35,516	32,199	19,078

We estimate the SPDs implied by these options (e.g., 31,794 SPDs for 1-month horizon) and run fixed-effect OLS regressions to test predictability, separately for each horizon:

$$R_{i,t+\tau} = \alpha_i + \beta x_{i,t,q,\tau} + \epsilon_{i,t} \tag{13}$$

where $R_{i,t+\tau}$ is firm i's return from t to $t+\tau$; $x_{i,t,q,\tau}$ is the qth-quantile of firm i's SPD for a maturity τ at t; and $\epsilon_{i,t}$ is the prediction error. To address cross-sectional dependence in returns, we apply a cross-sectional bootstrap to obtain 90% confidence intervals. For horizons longer than one month, we use a block cross-sectional bootstrap with a 12-month block size to account for serial correlation. Both methods are applied to the monthly horizon case as a robustness check. Further details can be found in the Appendix. Estimating quantile regressions with an unbalanced panel requires new methods and is beyond the scope of this paper.

Table 8: Predictive regression for stock returns using a quantile of the SPD as predictor

Quantile	0.10	0.20	0.30	0.40	0.50	0.60	0.70	0.80	0.90
(A) Maturity: 30 days									
Full sample: 1/1996-12/2021									
Estimate	-0.01	**0.95**	**0.39**	0.20	**0.55**	**0.85**	**1.10**	**0.99**	**0.56**
CI	[-0.27, 0.20]	[0.72, 1.20]	[0.27, 0.54]	[-0.08, 0.46]	[0.26, 0.85]	[0.59, 1.11]	[0.87, 1.37]	[0.78, 1.24]	[0.43, 0.74]
CI_B	[-0.32, 0.20]	[0.75, 1.26]	[0.22, 0.56]	[-0.12, 0.42]	[0.26, 0.78]	[0.65, 1.12]	[0.86, 1.49]	[0.73, 1.36]	[0.38, 0.80]
Subsample: 6/2009-2/2020									
Estimate	0.07	**0.70**	**0.42**	0.20	**0.42**	**0.62**	**0.83**	**0.84**	**0.55**
CI	[-0.11, 0.26]	[0.26, 1.11]	[0.28, 0.55]	[-0.05, 0.46]	[0.06, 0.77]	[0.19, 1.03]	[0.35, 1.22]	[0.46, 1.17]	[0.36, 0.73]
CI_B	[-0.09, 0.22]	[0.27, 1.07]	[0.26, 0.53]	[-0.05, 0.42]	[0.06, 0.75]	[0.21, 0.99]	[0.37, 1.2]	[0.42, 1.18]	[0.33, 0.72]
(B) Maturity: 91 days									
Full sample: 1/1996-12/2021									
Estimate	**-0.42**	0.05	**0.36**	-0.42	-0.35	-0.15	**0.47**	**0.76**	**0.55**
CI_B	[-0.92, -0.03]	[-0.26, 0.28]	[0.11, 0.67]	[-0.99, 0.01]	[-0.93, 0.09]	[-0.6, 0.19]	[0.03, 0.82]	[0.10, 1.37]	[0.14, 1.02]
Subsample: 6/2009-2/2020									
Estimate	**-0.41**	-0.08	**0.38**	**-0.44**	**-0.42**	-0.25	0.18	0.49	**0.53**
CI_B	[-0.55, -0.21]	[-0.42, 0.26]	[0.20, 0.49]	[-0.59, -0.22]	[-0.66, -0.14]	[-0.56, 0.08]	[-0.31, 0.39]	[-0.12, 0.79]	[0.26, 0.73]
(C) Maturity: 182 days									
Full sample: 1/1996-12/2021									
Estimate	**-0.76**	**-0.60**	**0.50**	**-0.80**	**-0.86**	**-0.78**	0.19	**1.02**	**0.76**
CI_B	[-1.43, -0.32]	[-1.31, -0.06]	[0.24, 0.90]	[-1.52, -0.31]	[-1.70, -0.27]	[-1.60, -0.17]	[-0.09, 0.39]	[0.40, 1.81]	[0.34, 1.36]
Subsample: 6/2009-2/2020									
Estimate	**-0.78**	**-0.64**	**0.47**	**-0.86**	**-0.94**	**-0.82**	0.17	**1.00**	**0.74**
CI_B	[-1.02, -0.46]	[-0.92, -0.27]	[0.22, 0.62]	[-1.10, -0.53]	[-1.20, -0.56]	[-1.09, -0.45]	[-0.30, 0.64]	[0.49, 1.53]	[0.47, 0.97]
(D) Maturity: 365 days									
Full sample: 1/1996-12/2021									
Estimate	**-1.19**	**-2.03**	**0.78**	**-1.22**	**-1.54**	**-1.88**	**-1.84**	-0.05	**1.02**
CI_B	[-2.13, -0.73]	[-3.36, -1.32]	[0.46, 1.37]	[-2.15, -0.79]	[-2.61, -1.03]	[-3.07, -1.25]	[-2.95, -1.06]	[-0.56, 0.65]	[0.64, 1.82]
Subsample: 6/2009-2/2020									
Estimate	**-0.81**	**-1.45**	**0.65**	**-0.86**	**-1.21**	**-1.42**	**-1.03**	0.31	**0.88**
CI_B	[-1.52, -0.10]	[-3.13, -0.48]	[0.15, 1.19]	[-1.66, -0.1]	[-2.42, -0.38]	[-2.94, -0.49]	[-2.7, -0.02]	[-0.47, 0.95]	[0.23, 1.54]

Note. Dependent variable: stock return. Independent variable: quantile of the SPD. CI (CI_B): 90% confidence interval using (block) cross-sectional bootstrap. Estimates significant at the 10% level are in bold.

Table 8 presents the results in four panels (A–D), each corresponding to a forecasting horizon. For the monthly horizon, seven of the nine estimates (each shown in a separate column, with significant estimates in bold) are statistically significant at the 10% level, and all are positive. The confidence intervals from the two bootstrap methods are similar, as expected if the regression residuals are serially uncorrelated. The two sample periods produce comparable point estimates and identical conclusions regarding statistical significance.

For the annual horizon, eight out of nine estimates are statistically significant, but unlike the monthly horizon, most of these estimates are negative. Recall that in the previous application, lower quantiles tended to produce negative estimates, while upper quantiles yielded positive estimates. This general pattern is also observed here, although more quantiles are now associated with negative estimates. Comparing estimates across all four horizons, we observe that the transition from positive to negative estimates generally occurs between the monthly and semi-annual horizons. Likely as a result of this transition, the estimates at the 3-month horizon have mixed signs, with many being statistically insignificant.

In summary, the results here suggest that the SPDs extracted from stock options have predictive power for future returns at both short (one month) and long (one year) horizons. The analysis also reveals a pattern of sign reversal when moving from short to longer horizons. Explaining this reversal requires additional data and can be a topic for future research.

6 Conclusion

This paper has introduced a new method for estimating state price densities implied by American-style options. The method involves estimating the parameters of a Gauss-Hermite series expansion and solving recursive equations for the early exercise premium. Because the method does not involve smoothing over time, it can capture sudden shifts in density that may occur during financial crises or in response to influential policy events. It also provides an estimate of the early exercise premium that is of independent interest. We examined the predictive power of the state price density implied by S&P 500 ETF options up to a one-year horizon using both mean and quantile regressions. The mean regressions indicate a significant predictive relationship between quantiles of the SPD and future expected returns when the 2008 financial crisis is excluded from the sample. The quantile regressions show clear patterns for horizons up to six months, where the quantiles above the median consistently demonstrate significant predictive power, irrespective of whether the 2008 financial crisis period is included in the sample. An application to individual stock options suggests that the SPDs have predictive power for future stock returns at both one month and one year horizons. The analysis also reveals a pattern of sign reversal when moving from short to longer horizon predictions that awaits further studies.

References

Aït-Sahalia, Y., and J. Duarte (2003): "Nonparametric option pricing under shape restrictions," *Journal of Econometrics*, 116(1-2), 9–47.

Aït-Sahalia, Y., and A. W. Lo (1998): "Nonparametric estimation of state-price densities implicit in financial asset prices," *The Journal of Finance*, 53(2), 499–547.

An, B.-J., A. Ang, T. G. Bali, and N. Cakici (2014): "The joint cross section of stocks and options," *The Journal of Finance*, 69(5), 2279–2337.

Andersen, T. G., N. Fusari, and V. Todorov (2015): "The risk premia embedded in index options," *Journal of Financial Economics*, 117(3), 558 – 584.

Andersen, T. G., V. Todorov, and M. Ubukata (2021): "Tail risk and return predictability for the Japanese equity market," *Journal of Econometrics*, 222(1, Part B), 344–363, Annals Issue: Financial Econometrics in the Age of the Digital Economy.

Andrews, D. W. (1991): "Heteroskedasticity and autocorrelation consistent covariance matrix estimation," *Econometrica*, 59(3), 827–858.

Bates, D. S. (2000): "Post-'87 crash fears in the S&P 500 futures option market," *Journal of Econometrics*, 94(1-2), 181–238.

Bates, D. S. (2012): "US stock market crash risk, 1926–2010," *Journal of Financial Economics*, 105(2), 229–259.

Bollerslev, T., M. Gibson, and H. Zhou (2011): "Dynamic estimation of volatility risk premia and investor risk aversion from option-implied and realized volatilities," *Journal of econometrics*, 160(1), 235–245.

Broadie, M., J. Detemple, E. Ghysels, and O. Torrès (2000): "American options with stochastic dividends and volatility: A nonparametric investigation," *Journal of Econometrics*, 94(1-2), 53–92.

Carlos Dias, J., and J. Pedro Vidal Nunes (2011): "Pricing real options under the constant elasticity of variance diffusion," *Journal of Futures Markets*, 31(3), 230–250.

Carr, P., R. Jarrow, and R. Myneni (1992): "Alternative characterizations of American put options," *Mathematical Finance*, 2(2), 87–106.

Cox, J. C. (1996): "The constant elasticity of variance option pricing model," *Journal of Portfolio Management*, 22, 15–17.

Dalderop, J. (2020): "Nonparametric filtering of conditional state-price densities," *Journal of Econometrics*, 214(2), 295–325.

Detemple, J., and W. Tian (2002): "The valuation of American options for a class of diffusion processes," *Management Science*, 48(7), 917–937.

Duffie, D., J. Pan, and K. Singleton (2000): "Transform analysis and asset pricing for affine jump-diffusions," *Econometrica*, 68(6), 1343–1376.

Fan, R., and J. H. Lee (2019): "Predictive quantile regressions under persistence and conditional heteroskedasticity," *Journal of Econometrics*, 213(1), 261–280, Annals: In Honor of Roger Koenker.

Figlewski, S. (2010): "Estimating the implied risk neutral density for the U.S. market portfolio," *Volatility and TimeSeries Econometrics: Essays in Honor of Robert F. Engle.*

Geman, H., and Y. F. Shih (2008): "Modeling commodity prices under the CEV model," *The Journal of Alternative Investments*, 11(3), 65–84.

Goyal, A., and A. Saretto (2009): "Cross-section of option returns and volatility," *Journal of Financial Economics*, 94(2), 310–326.

Gukhal, C. R. (2001): "Analytical valuation of American options on jump-diffusion processes," *Mathematical Finance*, 11(1), 97–115.

Gungor, S., and R. Luger (2021): "Exact inference in long-horizon predictive quantile regressions with an application to stock returns," *Journal of Financial Econometrics*, 19(4), 746–788.

Jacka, S. D. (1991): "Optimal stopping and the American put," *Mathematical Finance*, 1(2), 1–14.

Jackwerth, J. C., and M. Rubinstein (1996): "Recovering probability distributions from option prices," *Journal of Finance*, 51(5), 1611–32.

Jarrow, R., and A. Rudd (1982): "Approximate option valuation for arbitrary stochastic processes," *Journal of Financial Economics*, 10(3), 347–369.

Kim, I. J. (1990): "The analytic valuation of American options," *The Review of Financial Studies*, 3(4), 547–572.

Kim, I. J., and G. G. Yu (1996): "An alternative approach to the valuation of American options and applications," *Review of Derivatives Research*, 1, 61–85.

Lazarus, E., D. J. Lewis, J. H. Stock, and M. W. W. and (2018): "HAR inference: recommendations for practice," *Journal of Business & Economic Statistics*, 36(4), 541–559.

Longstaff, F. A. (1995): "Option pricing and the martingale restriction," *The Review of Financial Studies*, 8(4), 1091–1124.

Longstaff, F. A., and E. S. Schwartz (2001): "Valuing American options by simulation: a simple least-squares approach," *The review of financial studies*, 14(1), 113–147.

Lu, J., and Z. Qu (2021): "Sieve estimation of option-implied state price density," *Journal of Econometrics*, 224(1), 88–112.

Medvedev, A., and O. Scaillet (2010): "Pricing American options under stochastic volatility and stochastic interest rates," *Journal of Financial Economics*, 98(1), 145–159.

Melick, W. R., and C. P. Thomas (1997): "Recovering an asset's implied PDF from option prices: an application to crude oil during the gulf crisis," *Journal of Financial and Quantitative Analysis*, 32(1), 91–115.

Mencia, J., and E. Sentana (2013): "Valuation of VIX derivatives," *Journal of Financial Economics*, 108(2), 367–391.

Shimko, D. (1993): "Bounds of probability," *Risk*, 6, 33–37.

Tian, Y. S. (2011): "Extracting risk-neutral density and its moments from American option prices," *The Journal of Derivatives*, 18(3), 17–34.

Xing, Y., X. Zhang, and R. Zhao (2010): "What does the individual option volatility smirk tell us about future equity returns?," *Journal of Financial and Quantitative Analysis*, 45(3), 641–662.

Xiu, D. (2014): "Hermite polynomial based expansion of European option prices," *Journal of Econometrics*, 179(2), 158–177.

Estimating State Price Densities Implied by American Options Supplementary Appendix

Additional Details on the Simulation Design, Empirical Applications, and Tables and Figures

A.1 Additional details on the Simulation Design

This subsection provides details on the data generating processes used in the simulation analysis.

SV Model. We use the parameter values from the SV panel of Table 1 of Lu and Qu (2021), which are estimated using S&P500 options, with $r = 5\%$, $\delta = 2.5\%$, $\rho = -0.5268$, $S_t = 1300$, $\kappa = 4.2340$, $\theta = 0.0243$, $\sigma = 0.5121$, and $V_t = 0.0243$. The spans of the put and call strikes are both $[900, 1700]$, with 79 call and 79 put options.

Two-factor SV model. The parameters are taken from Bates (2000), with $\alpha_1 = 0.028, \alpha_2 = 0.130, \beta_1 = 0, \beta_2 = 5.58, \sigma_1 = 1.039, \sigma_2 = 0.667, \rho_1 = -0.775, \rho_2 = -0.382, V_{1,0} = 0.01, V_{2,0} = 0.01, r = 5\%$, and the initial value of the future price is set to $F_0 = 500$. The spans of the strikes for the put and call options are $[300, 800]$, generating 111 call and 111 put options.

DMR Model. The parameter values are taken from Table 4 in Mencia and Sentana (2013) and correspond to an empirical analysis of VIX derivative valuation models. These parameters were estimated using the sample period from March 2006 to August 2008, with $\beta = 2.575$, $\sigma = 3.732$, $\xi = 0.446$, $\alpha = 19.795$, and $\kappa = 1.360$ and the correlation between W and U is 0. The initial values of V_t and θ_t are set to 25. The risk-free rate is 5%. Under this DGP, the future price of V_t is given by (see Mencia and Sentana, 2013) $F(T) = \alpha + \delta(\tau)[\theta_t - \alpha] + exp(-\beta\tau)[V_t - \theta_t]$, where $\tau = T - t$, and $\delta(\tau) = (\beta/(\beta - \xi))exp(-\xi\tau) - (\xi/(\beta - \xi))exp(-\beta\tau)$. The implied spot price is $S(t) = exp(-r\tau)F(T)$. Using these formulas, we generate the data as follows. First, we simulate the V_t process. For each simulated V_t, we compute its future price $F(T)$ and discount it to obtain $S(t)$. As a result, for each simulated V_t process, we have an $S(t)$ process. We repeat this one million times and we obtain one million independent $S(t)$ process. Finally, we use these $S(t)$ as the underlying asset and obtain European and American option prices as we have done for other models, e.g., the SV model. The spans of the strikes for the put and call options are $[10, 100]$, with 51 call options and 51 put options.

CEV Model. The parameter values are taken from Geman and Shih (2009) for crude oil for the period 01/01/2000 to 12/11/2007, with $\delta = 0.025, \sigma = 0.19, \beta = 0.68$, and $V_0 = 100$. The spans of call and put option strikes are [10,250], with 57 calls and 57 puts.

SVCJ Model. Parameter values are taken from Lu and Qu (2021), estimated using S&P500 index options: $S_0 = 1300, V_0 = 0.0223, \theta = 0.0223, \kappa = 3.285, \sigma = 0.4084, \mu = 5.01e^{-4}, \rho = -0.6108, \lambda = 1.2775, \mu_s = -0.0308$, and $\sigma_s = 0.0248$. The spans of call and put option strikes are [900,1700], with 79 calls and 79 puts.

A.2 Additional Details on the Empirical Applications

A.2.1 Application to SPY options

The SPY series is designed to closely track the SPX; however, there are still some differences between the two. Below, we provide further details on these two series.

First, note that for our comparison of SPY and SPX estimates, the key factor is not their daily returns but whether their returns are similar at the horizons relevant to our analysis, specifically the 1-month to 1-year horizons. Differences in daily returns will only affect our analysis if they result in differences at these horizons. To investigate this, we compared the two return series at the 1-month, 3-month, 6-month, and 1-year horizons using QQ-plots. In Figure A.11, the x- and y-axes represent the returns of the two series. The results show that the returns closely follow the 45-degree line, indicating that these two series co-move closely at these horizons.

To further evaluate the size of the deviations from the 45-degree line, we computed the differences between SPX and SPY returns, standardized by the at-the-money (ATM) implied volatility of SPX options. This standardization allows the differences to be interpreted as approximate fractions of the return standard deviation, with small values indicating minor differences. The ATM implied volatility is calculated as the average of the implied volatilities of call and put options with strike prices closest to the spot price.

In Figure A.12, the circles represent the standardized return differences, with blue solid lines indicating the 5%-95% quantiles and red dotted lines the 1%-99% quantiles. The results show that 90% of the differences fall within 0.04 standard deviations of zero, and 98% are within 0.05. The maximum deviation is approximately 0.06 standard deviations. For an annualized implied volatility of 20%, this corresponds to a return of 20% $\times$ 0.06 = 1.2% at the annual horizon, which we consider small enough for our empirical comparison to be meaningful.

Another difference between the two series is that SPY pays quarterly dividends, which represent a delay in payout relative to SPX. However, for the sample period we consider, the annual dividend-yield on SPX has an average of 1.86% and a standard deviation of 0.44%. At the quarterly frequency and with an average of 1.5 month of average delay, this implies a difference in dividend-yield of about 1.86%/8=0.23%, which is a small value. Therefore, we can expect that the effect of this difference on the estimation to be small.

In an earlier stage of the paper, we also considered an alternative pair of options, OEX and XEO options, which are traded on the S&P 100 index and are American and European options, respectively. However, their market liquidity has declined significantly over time, to the point that there are no longer enough actively traded options to allow for proper estimation. For example, by the end of our sample period, the *monthly* aggregate trading volumes for XEO and OEX had dropped to 338 and 2,846 contracts, respectively. Also, we frequently observe negative early exercise premiums in the OEX/XEO sample. These negative values make the OEX/XEO combination problematic for assessing the early exercise premium which is supposed to be non-negative. For these reasons, we do not use this pair for our empirical comparisons.

This pattern is also documented in other studies. Lasser and Spizman (2016, Table 11) reported a sharp decline in OEX trading volume between 1999 and 2013, and remarked that "the OEX option trading volume has gone from around 50% of the trading volume in 1999 to a nearly nonexistent level today." Li et al. (2024) found that the mid-quote of an XEO option can be higher than that of an otherwise identical OEX option, implying a negative early exercise premium, and presented evidence that liquidity can explain this overpricing phenomenon. Their Figure 2 shows a dramatic decline in trading volumes from 2001 to 2021, especially for OEX.

A.2.2 Application to stock options

To present the cross-sectional bootstrap procedure, denote the original fixed-effect OLS estimate by $\hat{\beta}$. For any t, define $Y_{t,q,\tau}$ to include the observations from that period, as

$$Y_{t,q,\tau} = \{R_{i,t+\tau}, x_{i,t,q,\tau}\}\,.$$

First, take i.i.d. draws from the empirical distribution of $Y_{t,q,\tau}$, where $t = 1, \ldots, T$, to obtain a new sample denoted by $Y^*_{t,q,\tau}$ for $t = 1, \ldots, T$. Next, perform the fixed-effect OLS regression using this new sample to obtain an estimate for β; call it $\hat{\beta}^{*(1)}$. Repeat the sampling and estimation steps for $N = 10,000$ times and recenter the estimates around $\hat{\beta}$ to obtain $\{\hat{\beta}^{*(1)} - \hat{\beta}, \ldots, \hat{\beta}^{*(N)} - \hat{\beta}\}$. Obtain the 5th and 95th percentile of these values, and call them z^*_5 and z^*_{95}. Finally, a 90% confidence interval for β is computed as $[\hat{\beta} - z^*_{95}, \hat{\beta} - z^*_5]$.

For the block version of the cross-sectional bootstrap, we divide the data by year and resample from their empirical distribution. The rest of the procedure remains unchanged.

A.3 Figures and Tables

This subsection includes additional tables and figures for the simulation and empirical analyses in the paper.

Figure A.1: SPD and EEP estimates for the two-factor SV model

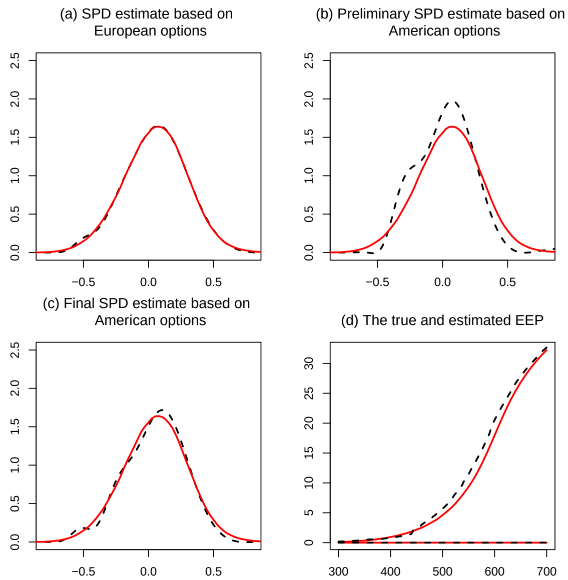

Note. Horizon: 1-year. Solid curve: true value. Dashed line: estimates. In (d), the increasing part is the put option EEP. See Appendix for more details about the DGP.

Figure A.2: SPD and EEP estimates for the DMR model

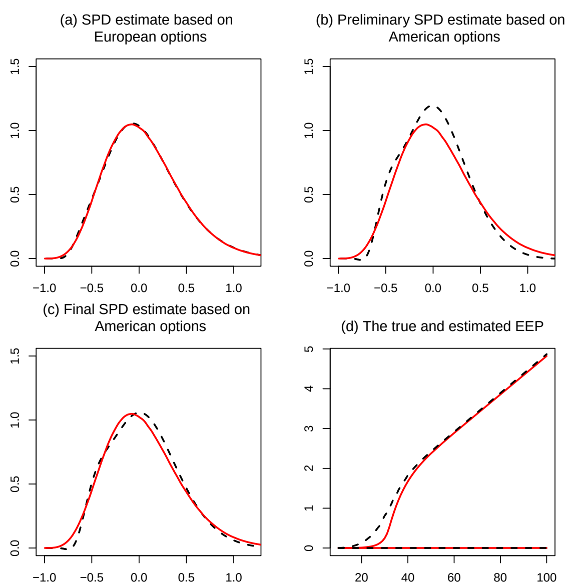

Note. 1-year horizon. Solid curve: true value. Dashed line: estimates. In (d), the increasing part is the put option EEP. See Appendix for more details about the DGP.

Figure A.3: SPD and EEP estimates for the CEV model

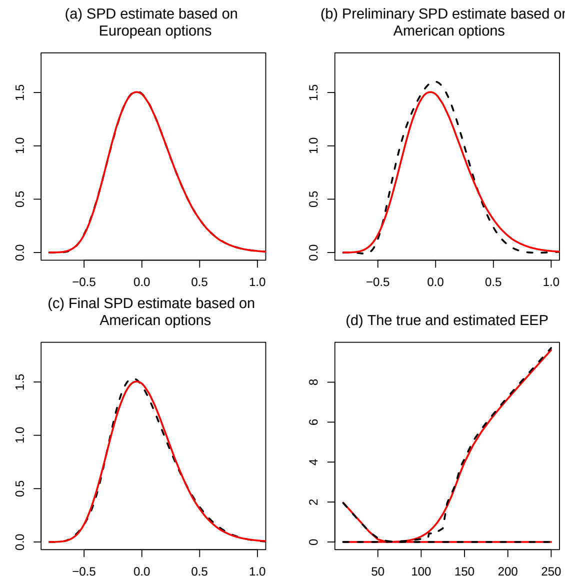

Note. 1-year horizon. Solid curve: true value. Dashed line: estimates. In (d), the increasing part is the put option EEP. See Appendix for more details about the DGP.

Figure A.4: SPD and EEP estimates for the SVCJ model

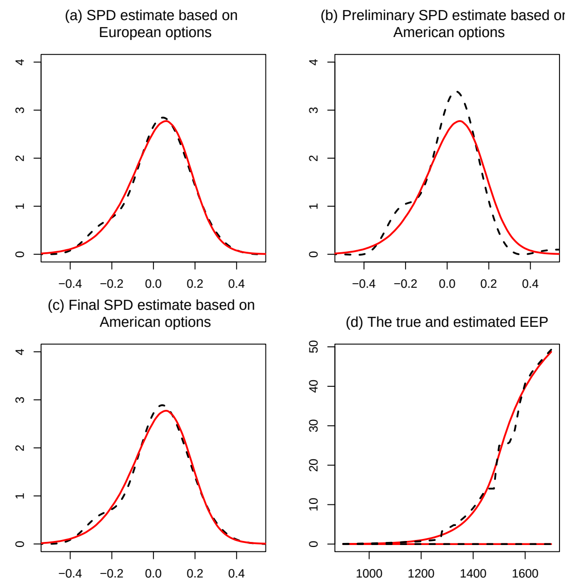

Note. 1-year horizon. Solid curve: true value. Dashed line: estimates. In (d), the increasing part is the put option EEP. See Appendix for more details about the DGP.

Figure A.5: SPD and EEP estimates for the SV model

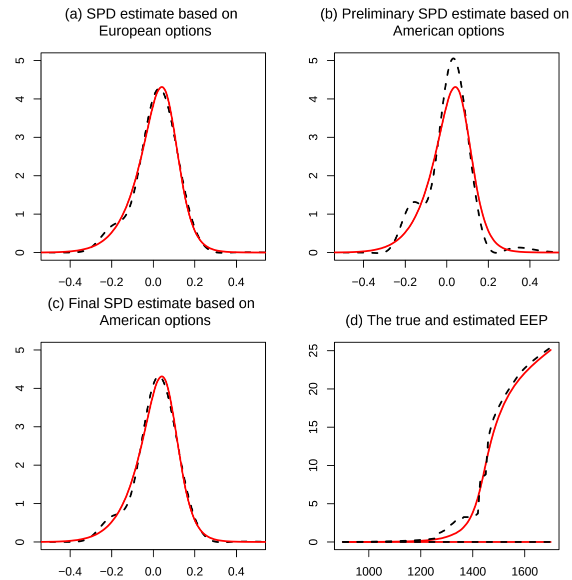

Note. Six-month horizon. Red curve represents the true value, and the dashed line corresponds to the estimate. In (d), the increasing function denotes the put option EEP. See the Appendix for more details about the DGP.

Figure A.6: SPD and EEP estimates for the two-factor SV model

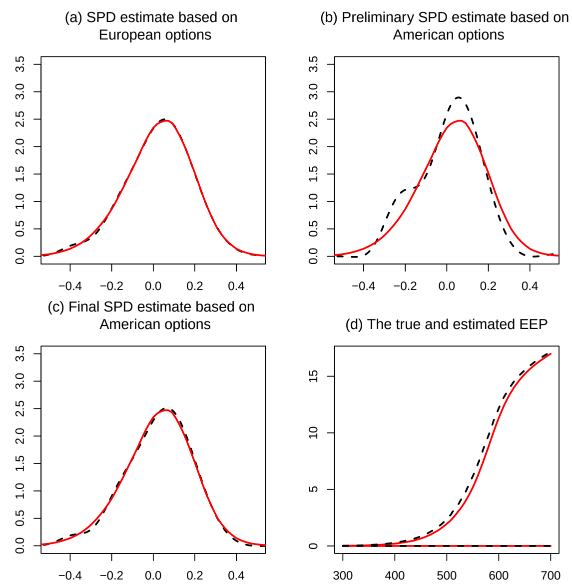

Note. Six-month horizon. Red curve represents the true value, and the dashed line corresponds to the estimate. In (d), the increasing function denotes the put option EEP. See the Appendix for more details about the DGP.

Figure A.7: SPD and EEP estimates for the DMR model

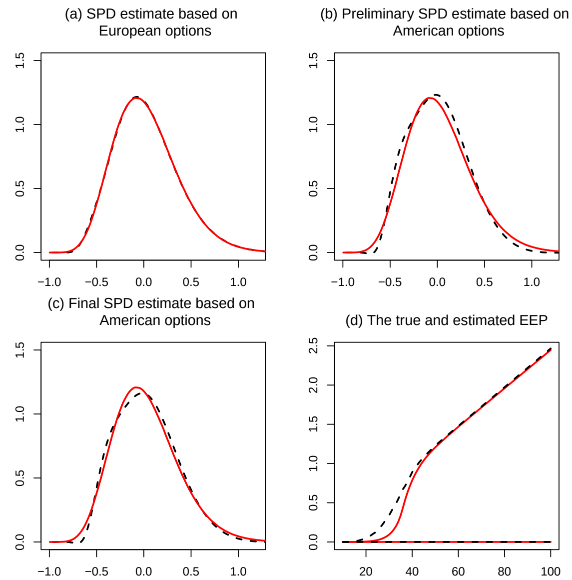

Note. Six-month horizon. Red curve represents the true value, and the dashed line corresponds to the estimate. In (d), the increasing function denotes the put option EEP. See the Appendix for more details about the DGP.

Figure A.8: SPD and EEP estimates for the CEV model

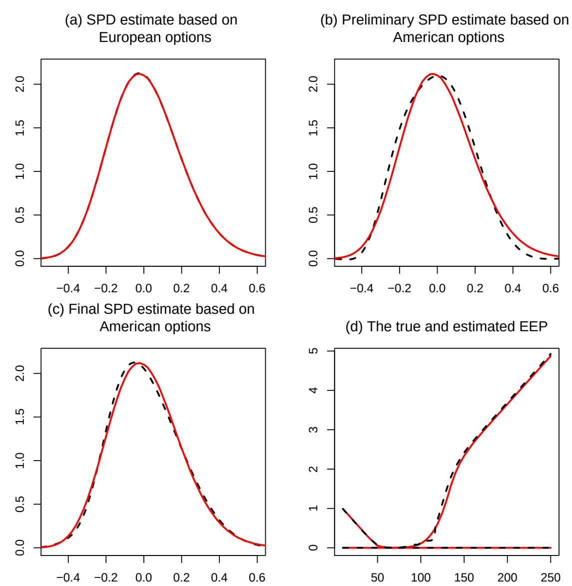

Note. Six-month horizon. Red curve represents the true value, and the dashed line corresponds to the estimate. In (d), the increasing function denotes the put option EEP. See the Appendix for more details about the DGP.

Figure A.9: SPD and EEP estimates for the SVCJ model

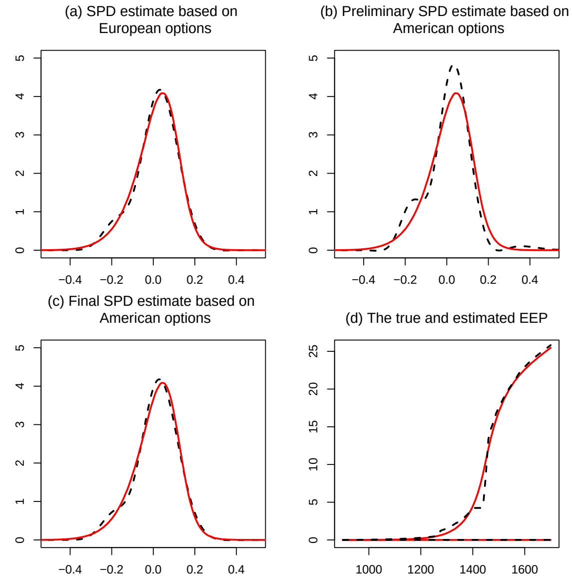

Note. Six-month horizon. Red curve represents the true value, and the dashed line corresponds to the estimate. In (d), the increasing function denotes the put option EEP. See the Appendix for more details about the DGP.

Figure A.10: SPX and SPY from 01/01/2007 to 02/28/2023

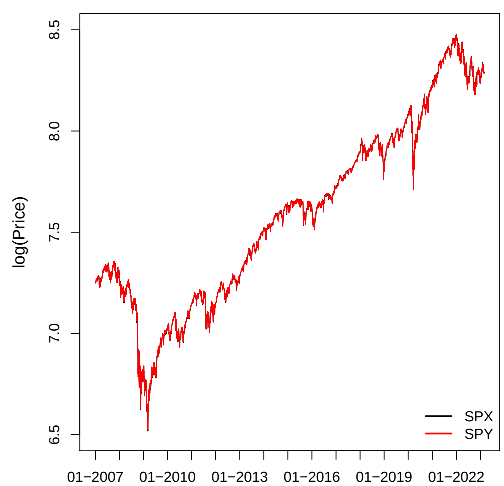

Note. Daily log price levels. SPY: the SPY ETF series; SPX: the S&P500 index. The SPY series is multipled by 10 before taking the log.

Figure A.11: QQ-Plot of returns of SPY vs SPX

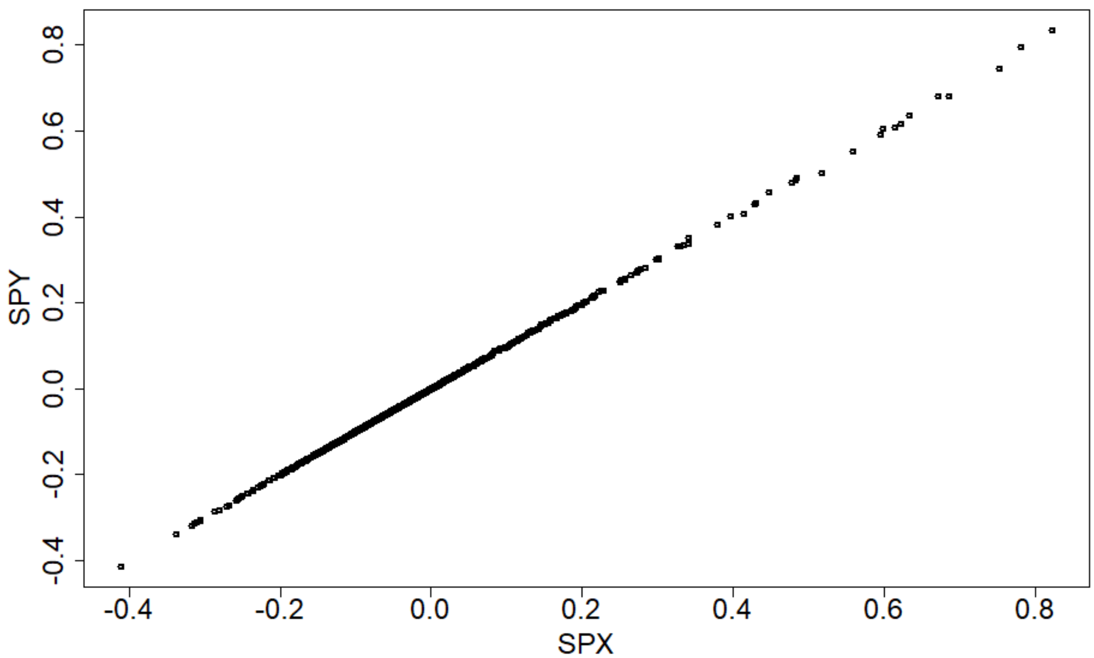

Figure A.12: IV-scaled Return Difference between SPX and SPY

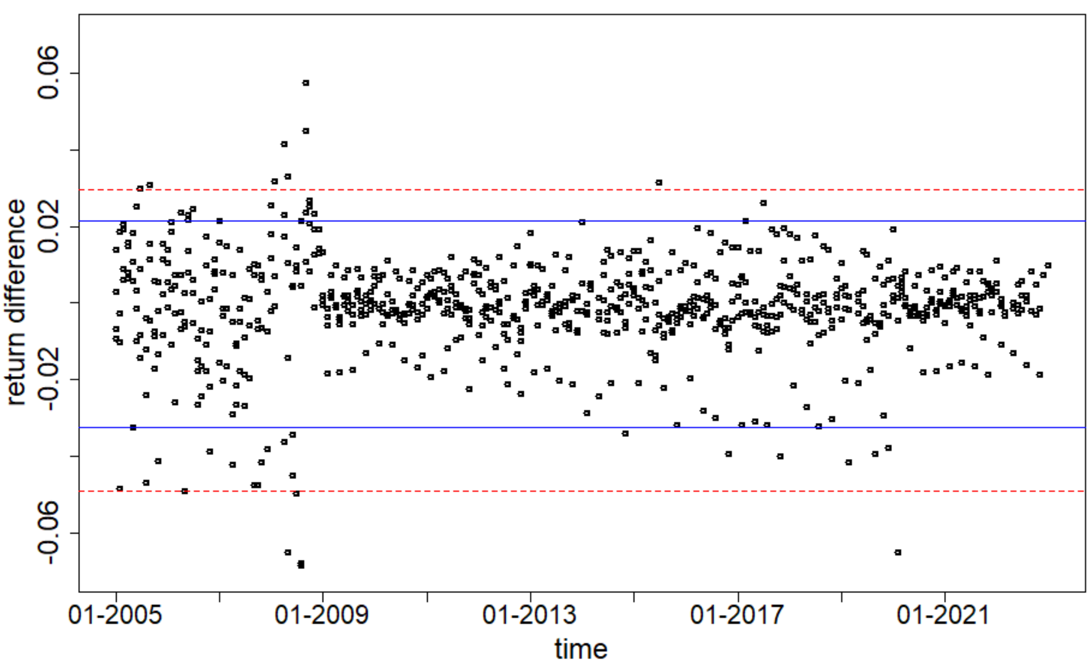

Figure A.13: SPD estimates for $\tau = 91$ days

(a) SPY ETF implied densities

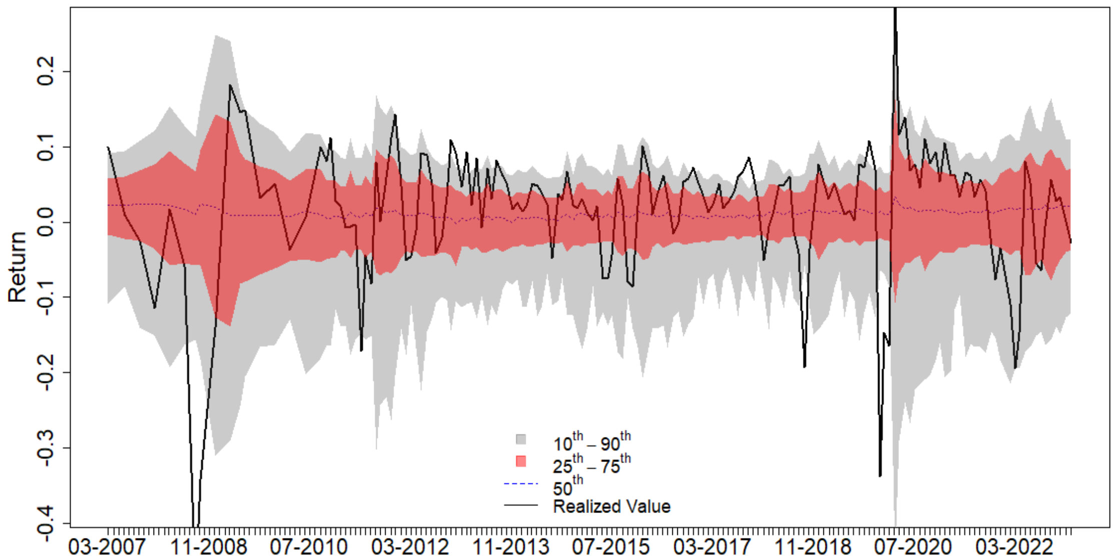

(b) SPX implied densities

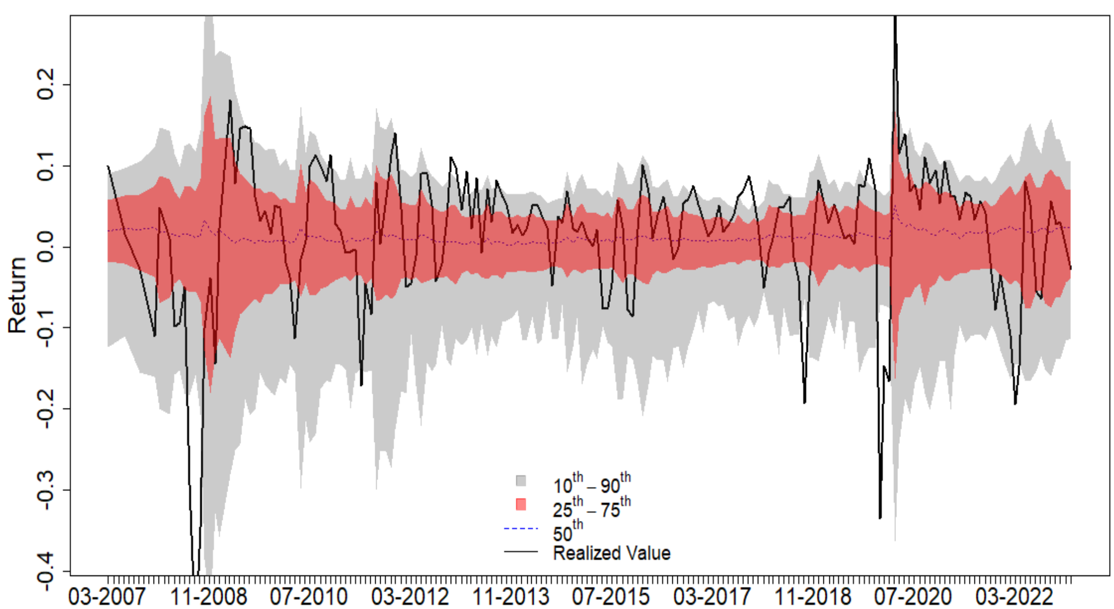

Figure A.14: SPD estimates for $\tau = 182$ days

(a) SPY ETF implied densities

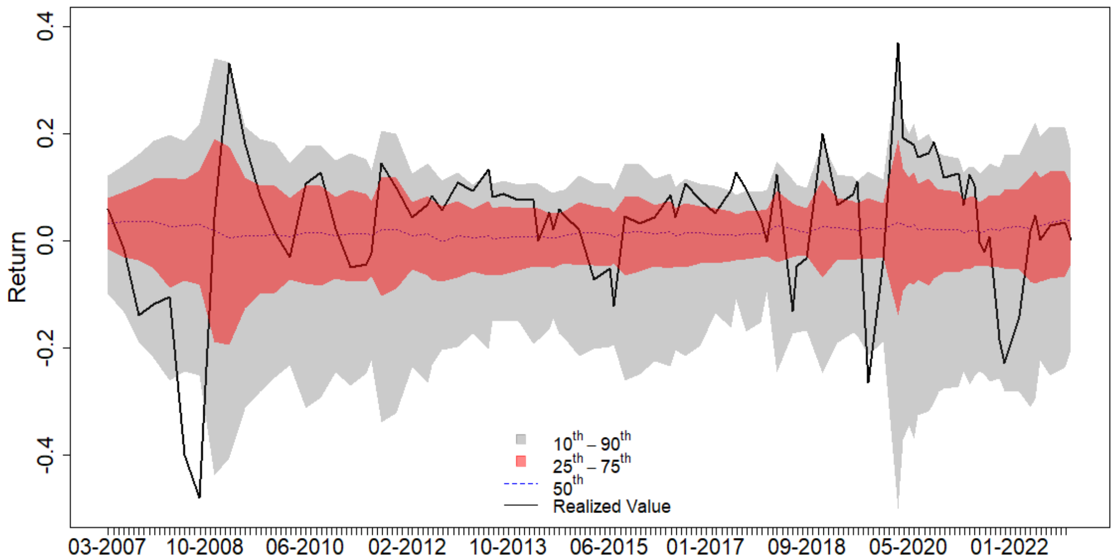

(b) SPX implied densities

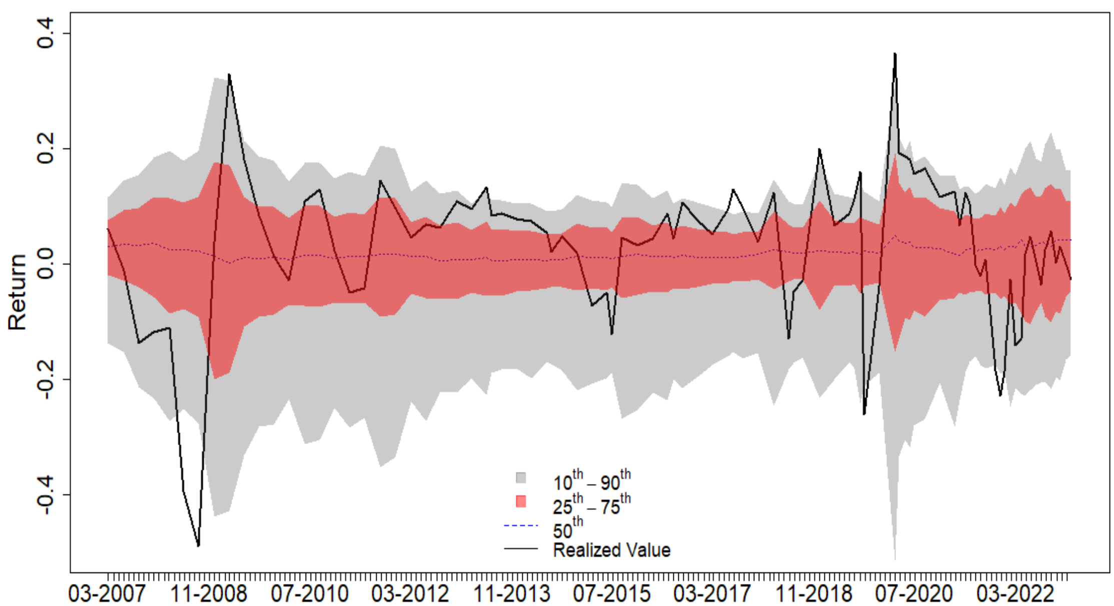

Figure A.15: SPD estimates for $\tau = 365$ days

(a) SPY ETF implied densities

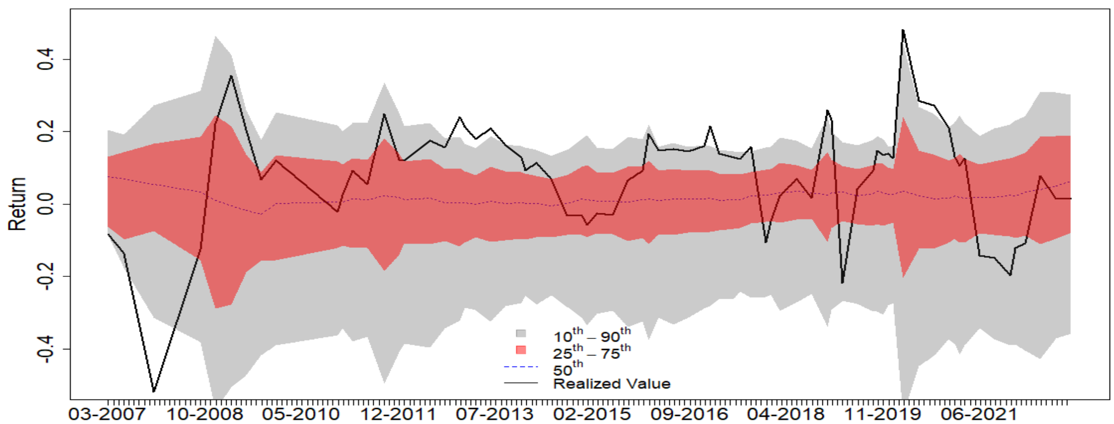

(b) SPX implied densities

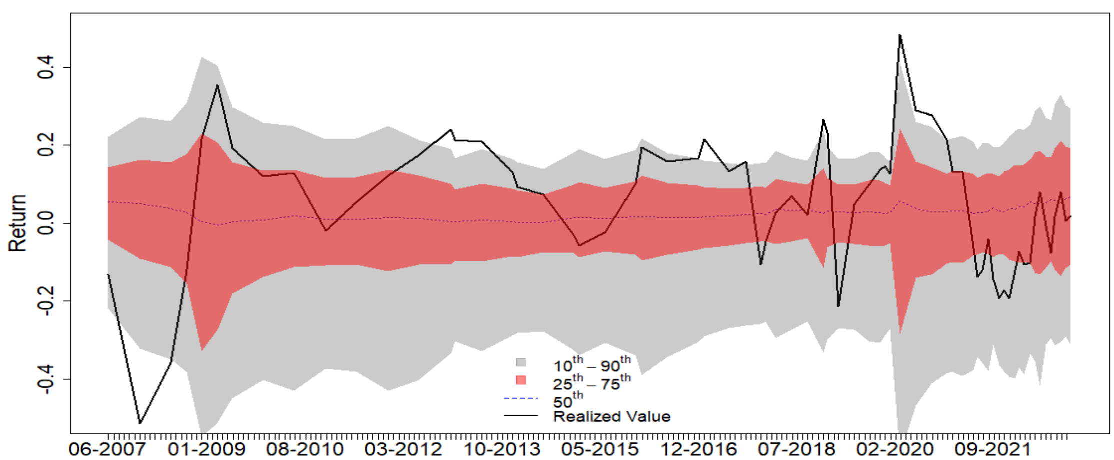

Table A.1: Predictive regression using a quantile of the SPD as the predictor: robustness check using fixed-b critical values.

Quantile	10	20	30	40	50	60	70	80	90
Maturity: 30 days									
(a) 06/2009–02/2020									
test	**13.91**	**10.11**	**7.50**	**4.32**	1.98	**15.54**	**16.15**	**17.61**	**17.71**
cv	3.52	3.52	3.52	3.52	3.52	3.52	3.52	3.52	3.52
(b) 06/2009–02/2023									
test	**14.61**	**23.25**	**10.91**	**5.49**	2.35	**6.12**	**8.18**	**10.01**	**10.43**
cv	3.44	3.44	3.44	3.44	3.44	3.44	3.44	3.44	3.44
(c) 01/2007–02/2023									
test	1.47	3.05	2.66	**3.97**	0.09	0.96	1.55	1.76	1.93
cv	3.40	3.40	3.40	3.40	3.40	3.40	3.40	3.40	3.40
Maturity: 91 days									
(a) 06/2009–02/2020									
test	**5.76**	**10.04**	**10.94**	**14.32**	0.02	**3.81**	**7.08**	**7.73**	**7.87**
cv	3.60	3.60	3.60	3.60	3.60	3.60	3.60	3.60	3.60
(b) 06/2009–02/2023									
test	**4.73**	**6.94**	**7.52**	**12.72**	0.26	1.96	3.28	**4.09**	**4.68**
cv	3.48	3.48	3.48	3.48	3.48	3.48	3.48	3.48	3.48
(c) 01/2007–02/2023									
test	2.65	1.52	2.34	**5.53**	0.03	0.33	0.69	0.90	1.04
cv	3.44	3.44	3.44	3.44	3.44	3.44	3.44	3.44	3.44
Maturity: 182 days									
(a) 06/2009–02/2020									
test	3.62	**9.32**	**9.80**	**11.06**	0.39	1.70	**5.86**	**6.97**	**7.47**
cv	4.07	4.07	4.07	4.07	4.07	4.07	4.07	4.07	4.07
(b) 06/2009–02/2023									
test	3.76	**14.25**	**8.14**	**7.40**	0.15	1.66	2.82	3.50	**4.50**
cv	3.81	3.81	3.81	3.81	3.81	3.81	3.81	3.81	3.81
(c) 01/2007–02/2023									
test	**4.26**	**6.07**	**8.88**	**41.35**	0.73	0.04	0.51	1.03	1.50
cv	3.77	3.77	3.77	3.77	3.77	3.77	3.77	3.77	3.77
Maturity: 365 days									
(a) 06/2009–02/2020									
test	**7.27**	**10.18**	**5.66**	3.60	1.02	0.41	**6.15**	**7.15**	**6.93**
cv	4.16	4.16	4.16	4.16	4.16	4.16	4.16	4.16	4.16
(b) 06/2009–02/2023									
test	2.34	**32.21**	**8.98**	**6.29**	0.97	0.12	0.82	1.29	1.94
cv	3.93	3.93	3.93	3.93	3.93	3.93	3.93	3.93	3.93
(c) 01/2007–02/2023									
test	**9.59**	**46.54**	**29.29**	**31.75**	**7.67**	0.40	0.19	1.02	2.48
cv	3.93	3.93	3.93	3.93	3.93	3.93	3.93	3.93	3.93

Note. test: the squared t test using Newey–West standard errors with a large bandwidth $S = 1.3T^{1/2}$, recommended in Lazarus et al. (2018). cv: fixed-b critical values. The tests and critical values are computed using the accompanying MATLAB code of Lazarus et al. (2018). Bold indicates significance at the 10% level.

Table A.2: Predictive regression using a quantile of the SPD as the predictor: robustness check using an equally weighted Cosine estimator of the long run variance.

Quantile	10	20	30	40	50	60	70	80	90
Maturity: 30 days									
(a) 06/2009–02/2020									
test	**9.20**	**8.14**	**5.87**	3.07	1.58	**13.47**	**13.67**	**14.73**	**14.89**
cv	3.29	3.29	3.29	3.29	3.29	3.29	3.29	3.29	3.29
(b) 06/2009–02/2023									
test	**13.07**	**21.79**	**10.47**	**5.36**	1.90	**5.54**	**7.41**	**9.11**	**9.52**
cv	3.18	3.18	3.18	3.18	3.18	3.18	3.18	3.18	3.18
(c) 01/2007–02/2023									
test	1.37	2.82	2.47	**3.73**	0.09	0.89	1.42	1.61	1.77
cv	3.14	3.14	3.14	3.14	3.14	3.14	3.14	3.14	3.14
Maturity: 91 days									
(a) 06/2009–02/2020									
test	**3.79**	**8.14**	**9.00**	**12.97**	0.02	**3.44**	**5.60**	**5.95**	**5.93**
cv	3.36	3.36	3.36	3.36	3.36	3.36	3.36	3.36	3.36
(b) 06/2009–02/2023									
test	**4.05**	**6.56**	**7.33**	**15.61**	0.21	1.74	2.97	**3.73**	**4.29**
cv	3.23	3.23	3.23	3.23	3.23	3.23	3.23	3.23	3.23
(c) 01/2007–02/2023									
test	2.33	1.43	2.22	**4.71**	0.03	0.29	0.63	0.83	0.96
cv	3.18	3.18	3.18	3.18	3.18	3.18	3.18	3.18	3.18
Maturity: 182 days									
(a) 06/2009–02/2020									
test	3.64	**7.09**	**6.44**	**8.18**	0.66	1.71	**8.33**	**9.31**	**9.41**
cv	4.06	4.06	4.06	4.06	4.06	4.06	4.06	4.06	4.06
(b) 06/2009–02/2023									
test	2.66	**11.26**	**6.08**	**7.11**	0.11	1.19	2.07	2.60	3.37
cv	3.59	3.59	3.59	3.59	3.59	3.59	3.59	3.59	3.59
(c) 01/2007–02/2023									
test	3.07	**5.07**	**7.82**	**50.22**	0.63	0.03	0.39	0.78	1.16
cv	3.46	3.46	3.46	3.46	3.46	3.46	3.46	3.46	3.46
Maturity: 365 days									
(a) 06/2009–02/2020									
test	**9.24**	**7.34**	3.49	2.12	0.71	0.47	**6.07**	**7.11**	**6.75**
cv	4.06	4.06	4.06	4.06	4.06	4.06	4.06	4.06	4.06
(b) 06/2009–02/2023									
test	1.53	**31.12**	**5.28**	3.15	0.53	0.06	0.44	0.71	1.10
cv	3.78	3.78	3.78	3.78	3.78	3.78	3.78	3.78	3.78
(c) 01/2007–02/2023									
test	**6.14**	**50.21**	**31.66**	**18.59**	**3.88**	0.22	0.12	0.65	**1.66**
cv	3.59	3.59	3.59	3.59	3.59	3.59	3.59	3.59	3.59

Note. test: the squared t test using Müller's (2004) equally weighted Cosine estimator of the long-run variance, with the number of Cosine terms set to $v = 0.4T^{2/3}$, as recommended in Lazarus et al. (2018). cv: critical values from F distributions. The tests and critical values are computed using the accompanying MATLAB code of Lazarus et al. (2018). Bold indicates significance at the 10% level.

Table A.3: Quantile regression using a quantile of the SPD as the predictor (τ=30 days)

Quantile	0.10	0.20	0.30	0.40	0.50	0.60	0.70	0.80	0.90
(a) 06/2009-02/2020									
Estimate	-0.56	-0.28	-0.73	-0.63	1.69	1.77	1.68	1.10	0.65
s.e.	0.20	0.67	0.76	0.79	1.02	0.66	0.35	0.06	0.11
t-value	-2.83	-0.41	-0.96	-0.80	1.66	2.70	4.83	18.82	5.94
p-value	**0.00**	0.68	0.34	0.43	**0.10**	**0.01**	**0.00**	**0.00**	**0.00**
(b) 06/2009-02/2023									
Estimate	-0.61	-0.36	-0.84	-1.06	1.43	1.77	1.57	1.13	0.78
s.e.	0.29	0.53	0.59	0.52	0.89	0.53	0.42	0.28	0.26
t-value	-2.13	-0.67	-1.42	-2.04	1.61	3.34	3.75	4.01	2.99
p-value	**0.03**	0.50	0.15	**0.04**	0.11	**0.00**	**0.00**	**0.00**	**0.00**
(c) 01/2007-02/2023									
Estimate	0.39	0.29	0.06	-0.76	1.36	1.21	1.22	0.97	0.70
s.e.	0.26	0.39	0.85	0.91	0.82	0.41	0.31	0.18	0.10
t-value	1.47	0.73	0.07	-0.84	1.66	2.93	3.97	5.30	7.00
p-value	0.16	0.46	0.94	0.40	**0.10**	**0.00**	**0.00**	**0.00**	**0.00**

Note. The standard errors allow for heteroscedasticity and autocorrelation. The estimates that are significant at the 10% level are in bold.

Table A.4: Quantile regression using a quantile of the SPD as the predictor (τ=91 days)

Quantile	0.10	0.20	0.30	0.40	0.50	0.60	0.70	0.80	0.90
(a) 06/2009-02/2020									
Estimate	-0.64	-1.03	-1.32	-1.55	0.68	1.66	1.58	1.12	0.96
s.e.	0.45	0.68	0.91	1.52	1.14	0.63	0.49	0.41	0.30
t-value	-1.40	-1.52	-1.45	-1.02	0.60	2.62	3.25	2.70	3.23
p-value	0.16	0.13	0.15	0.31	0.55	**0.01**	**0.00**	**0.01**	**0.00**
(b) 06/2009-02/2023									
Estimate	-0.61	-1.13	-1.49	-2.71	1.44	1.87	1.39	1.11	1.08
s.e.	0.66	0.48	0.82	1.57	1.54	0.82	0.67	0.47	0.48
t-value	-0.93	-2.36	-1.81	-1.73	0.94	2.29	2.08	2.37	2.25
p-value	0.35	**0.02**	**0.07**	**0.08**	0.35	**0.02**	**0.04**	**0.02**	**0.02**
(c) 01/2007-02/2023									
Estimate	0.36	-0.48	-1.14	-2.83	0.06	1.63	1.42	1.10	0.98
s.e.	0.45	0.92	0.86	1.00	1.32	0.78	0.44	0.42	0.30
t-value	0.80	-0.52	-1.33	-2.83	0.05	2.10	3.21	2.62	3.33
p-value	0.42	0.60	0.18	**0.00**	0.96	**0.04**	**0.00**	**0.01**	**0.00**

Note. The standard errors allow for heteroscedasticity and autocorrelation. The estimates that are significant at the 10% level are in bold.

Table A.5: Quantile regression using a quantile of the SPD as the predictor (τ=182 days)

Quantile	0.10	0.20	0.30	0.40	0.50	0.60	0.70	0.80	0.90
				(a) 06/2009-02/2020					
Estimate	-0.03	-0.59	-2.21	-3.90	0.40	1.96	1.53	1.20	0.72
s.e.	0.60	0.67	1.23	1.67	2.16	1.09	0.70	0.54	0.61
t-value	-0.06	-0.88	-1.80	-2.34	0.19	1.80	2.20	2.22	1.18
p-value	0.95	0.38	**0.07**	**0.02**	0.85	**0.07**	**0.03**	**0.03**	0.24
				(b) 06/2009-02/2023					
Estimate	-0.67	-1.33	-2.21	-4.13	-0.48	2.69	1.97	1.41	1.17
s.e.	0.73	0.78	0.73	1.31	2.28	1.62	0.63	0.38	0.30
t-value	-0.93	-1.70	-3.04	-3.14	-0.21	1.66	3.13	3.75	3.91
p-value	0.35	**0.09**	**0.00**	**0.00**	0.83	**0.10**	**0.00**	**0.00**	**0.00**
				(c) 01/2007-02/2023					
Estimate	-0.31	-0.43	-1.99	-4.27	-1.14	1.73	1.96	1.57	1.05
s.e.	1.37	0.56	1.10	0.84	1.27	1.60	0.76	0.27	0.20
t-value	-0.23	-0.76	-1.81	-5.10	-0.90	1.08	2.58	5.80	5.14
p-value	0.82	0.45	**0.07**	**0.00**	0.37	0.28	**0.01**	**0.00**	**0.00**

Note. The standard errors allow for heteroscedasticity and autocorrelation. The estimates that are significant at the 10% level are in bold.

Table A.6: Quantile regression using a quantile of the SPD as the predictor (τ=365 days)

Quantile	0.10	0.20	0.30	0.40	0.50	0.60	0.70	0.80	0.90
				(a) 06/2009-02/2020					
Estimate	-0.96	-1.10	-1.19	-0.90	0.27	0.67	1.41	0.80	0.91
s.e.	0.44	0.34	1.11	1.46	1.76	1.18	0.90	0.64	0.61
t-value	-2.16	-3.25	-1.07	-0.62	0.15	0.57	1.57	1.24	1.50
p-value	**0.03**	**0.00**	0.28	0.54	0.88	0.57	0.12	0.21	0.13
				(b) 06/2009-02/2023					
Estimate	-0.80	-1.17	-1.43	-1.18	0.67	2.38	2.75	1.83	1.07
s.e.	0.87	0.60	0.89	1.48	1.58	1.34	1.17	0.62	0.62
t-value	-0.92	-1.95	-1.60	-0.80	0.42	1.78	2.36	2.94	1.72
p-value	0.36	**0.05**	0.11	0.43	0.67	**0.07**	**0.02**	**0.00**	**0.09**
				(c) 01/2007-02/2023					
Estimate	-0.07	-1.18	-1.94	-2.22	-2.57	-1.34	1.42	1.31	1.07
s.e.	0.46	0.19	0.38	0.74	1.61	1.58	0.91	0.65	0.18
t-value	-0.14	-6.17	-5.09	-2.99	-1.60	-0.85	1.56	2.01	5.83
p-value	0.89	**0.00**	**0.00**	**0.00**	0.11	0.40	0.12	**0.04**	**0.00**

Note. The standard errors allow for heteroscedasticity and autocorrelation. The estimates that are significant at the 10% level are in bold.

Table A.7: Quantile regression using a quantile of the SPD as the predictor (τ=30 days): robustness check using Fan and Lee's (2019) methods

Quantile	0.10	0.20	0.30	0.40	0.50	0.60	0.70	0.80	0.90
(a) 06/2009-02/2020									
Estimate	-0.71	0.22	-0.70	-0.88	1.92	**1.42**	1.20	**0.73**	**0.66**
CI:LB	-0.94	-1.52	-2.61	-2.47	-0.60	0.11	-0.07	0.02	0.23
CI:UB	1.11	1.51	1.55	0.70	3.43	2.44	2.14	1.84	1.08
(b) 06/2009-02/2023									
Estimate	-0.69	0.50	-0.10	-1.01	2.00	**1.75**	**1.22**	**1.01**	**0.85**
CI:LB	-0.83	-0.95	-1.97	-3.91	-0.05	0.50	0.16	0.19	0.28
CI:UB	0.86	1.30	2.10	0.29	3.56	2.91	1.76	1.28	0.81
(c) 01/2007-02/2023									
Estimate	0.14	0.40	0.26	0.63	0.63	1.47	**1.14**	**0.77**	**0.67**
CI:LB	-0.66	-0.97	-1.94	-2.36	-1.14	-0.52	0.09	0.11	0.35
CI:UB	1.02	1.43	2.94	2.07	2.14	2.30	1.74	1.11	0.79

Note: The slope coefficient estimates and their 90% bootstrap confidence intervals [CI:LB, CI:UB] are computed using the methods of Fan and Lee (2019). The horizon is at 30 days as their approach is for single-horizon forecasts only. Significant estimates are highlighted in bold.

Table A.8: Quantile regression using a quantile of the SPD as the predictor (τ=30 days): robustness check based on Gungor and Luger's (2021) approach

Quantile	0.10	0.20	0.30	0.40	0.50	0.60	0.70	0.80	0.90
(a) 01/2009-02/2020									
t-stat	-1.96	-0.35	-1.00	-0.78	1.68	2.85	**4.79**	**18.49**	**7.13**
CI:LB	-2.11	-1.64	-1.81	-1.62	-1.61	-1.32	-1.58	-1.21	-1.60
CI:UB	1.53	1.64	1.58	1.31	2.14	3.36	2.86	2.64	2.70
(b) 01/2009-02/2023									
t-stat	-1.50	-0.53	-1.22	-1.97	1.63	3.32	**4.37**	**5.14**	**5.35**
CI:LB	-2.56	-2.19	-1.99	-1.70	-1.64	-1.47	-1.57	-1.14	-1.49
CI:UB	1.64	2.21	1.95	1.51	2.06	3.55	3.22	2.81	3.49
(c) 01/2007-02/2023									
t-stat	0.88	0.62	0.07	-0.82	1.66	2.77	**4.03**	**5.64**	**9.03**
CI:LB	-1.51	-2.06	-2.31	-1.88	-1.54	-1.61	-1.55	-0.89	-1.13
CI:UB	2.30	2.35	2.07	1.58	2.51	3.57	3.64	3.29	4.28

The t-statistics for the slope coefficient and the 90% confidence intervals [CI:LB, CI:UB] under the null hypothesis of no predictability are computed using a variation of Gungor and Luger's (2021) procedure. First, a 98% confidence interval for the autoregressive coefficient of the predictor is obtained by inverting a unit root test. Then, a 92% bootstrap confidence interval for the t-statistic in the predictive regression is calculated for the least favorable value within this interval. The t-statistics are computed assuming independent, non-identically distributed errors, and the 90% bootstrap confidence intervals are derived using the same method to ensure bootstrap consistency. Significant values are highlighted in bold.

Table A.9: Quantile regression using a quantile of the SPD as the predictor (τ=91 days): robustness check based on Gungor and Luger's (2021) approach

Quantile	0.10	0.20	0.30	0.40	0.50	0.60	0.70	0.80	0.90
				(a) 01/2009-02/2020					
t-stat	**-2.10**	-1.67	-1.53	-1.13	0.58	2.08	**3.26**	**3.18**	**4.31**
CI:LB	-1.91	-1.95	-1.71	-1.50	-1.61	-1.78	-1.51	-1.61	-1.74
CI:UB	1.42	1.72	1.48	1.39	1.96	2.36	2.27	2.16	2.13
				(b) 01/2009-02/2023					
t-stat	-1.43	**-3.38**	**-2.26**	-2.23	1.50	**3.53**	**3.44**	**3.70**	**5.03**
CI:LB	-2.35	-2.19	-1.91	-1.71	-1.76	-1.81	-1.43	-1.58	-1.71
CI:UB	1.48	1.77	1.53	1.36	1.97	2.61	2.81	2.50	2.43
				(c) 01/2007-02/2023					
t-stat	1.05	-0.66	-1.21	**-2.61**	0.06	**2.71**	**3.92**	**3.99**	**5.44**
CI:LB	-1.97	-1.95	-1.78	-1.50	-1.81	-1.89	-1.52	-1.81	-1.91
CI:UB	1.99	2.40	2.00	1.60	1.83	2.47	3.18	2.95	3.85

See Table A.8.

Table A.10: Quantile regression using a quantile of the SPD as the predictor (τ=182 days): robustness check based on Gungor and Luger's (2021) approach

Quantile	0.10	0.20	0.30	0.40	0.50	0.60	0.70	0.80	0.90
				(a) 01/2009-02/2020					
t-stat	-0.03	-0.95	-1.94	**-2.51**	0.22	1.85	2.28	2.71	2.16
CI:LB	-2.24	-1.93	-2.00	-1.64	-1.29	-1.26	-0.99	-0.94	-0.98
CI:UB	1.60	1.66	1.71	1.67	2.57	3.14	3.20	3.26	3.77
				(b) 01/2009-02/2023					
t-stat	-0.09	-1.60	**-3.42**	**-3.49**	-0.31	2.82	**5.31**	**5.41**	**7.45**
CI:LB	-2.00	-2.03	-2.02	-1.75	-1.53	-1.41	-1.30	-1.31	-1.45
CI:UB	1.90	1.52	1.55	1.64	2.17	2.83	3.04	3.37	4.08
				(c) 01/2007-02/2023					
t-stat	-0.25	-0.60	-1.62	**-3.73**	-0.53	1.90	**3.85**	**7.54**	**8.03**
CI:LB	-1.58	-2.04	-1.96	-1.81	-1.52	-1.59	-1.53	-1.61	-1.52
CI:UB	1.81	1.83	1.72	1.74	2.15	2.46	3.07	3.81	4.87

See Table A.8.

Table A.11: Quantile regression using a quantile of the SPD as the predictor (τ=365 days): robustness check based on Gungor and Luger's (2021) approach

Quantile	0.10	0.20	0.30	0.40	0.50	0.60	0.70	0.80	0.90
					(a) 01/2009-02/2020				
t-stat	-2.10	**-2.58**	-1.50	-0.71	0.20	0.54	1.64	1.66	1.82
CI:LB	-2.15	-2.19	-2.02	-1.84	-1.51	-1.26	-1.18	-1.33	-1.56
CI:UB	1.89	1.75	1.71	1.58	1.65	2.54	3.22	3.27	3.79
					(b) 01/2009-02/2023				
t-stat	0.55	-2.44	-2.08	-1.61	-1.57	0.07	**2.53**	**3.95**	**4.77**
CI:LB	-2.22	-2.99	-2.21	-2.05	-1.72	-1.48	-1.47	-1.58	-1.60
CI:UB	2.17	1.70	1.62	1.54	1.45	1.49	2.36	2.83	3.76
					(c) 01/2007-02/2023				
t-stat	-0.09	**-5.43**	-4.78	-2.69	**-2.54**	-1.24	2.05	3.11	**8.80**
CI:LB	-1.44	-3.70	-6.19	-4.48	-2.36	-1.88	-1.73	-1.66	-1.28
CI:UB	2.53	2.26	1.71	1.57	1.42	1.44	2.79	3.29	7.38

See Table A.8.

References

Lasser, D. J., and J. D. Spizman (2016): "The Value of the Wildcard Option in Cash-settled American Index Options," *Journal of Financial Markets*, 28, 116–131.

Lazarus, E., D. J. Lewis, J. H. Stock, and M. W. Watson (2018). "HAR Inference: Recommendations for Practice," *Journal of Business & Economic Statistics* 36, 541-559.

Li, W., J. E. Zhang, X. Ruan, and P. Aschakulporn (2024): "An Empirical Study on the Early Exercise Premium of American Options: Evidence from OEX and XEO Options," *The Journal of Futures Markets*, 44, 1117–1153.

Müller, U. K. (2004). A Theory of Robust Long-Run Variance Estimation. *Working paper*, Princeton University.